

g  
2

AFFDL-TR-77-37

88  
58  
35  
05  
AD A 053588

# DIGITAL SIMULATION OF FLEXIBLE AIRCRAFT RESPONSE TO SYMMETRICAL AND ASYMMETRICAL RUNWAY ROUGHNESS

Anthony G. Gerardi

Structural Integrity Branch  
Structural Mechanics Division

August 1977

TECHNICAL REPORT AFFDL-TR-77-37

DDC FILE COPY

Approved for public release; distribution unlimited.



AIR FORCE FLIGHT DYNAMICS LABORATORY  
AIR FORCE WRIGHT AERONAUTICAL LABORATORIES  
AIR FORCE SYSTEMS COMMAND  
WRIGHT-PATTERSON AIR FORCE BASE, OHIO 45433

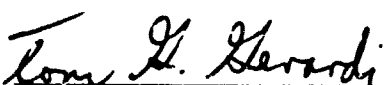
**Best  
Available  
Copy**

NOTICE

When Government drawings, specifications, or other data are used for any purpose other than in connection with a definitely related Government procurement operation, the United States Government thereby incurs no responsibility nor any obligation whatsoever; and the fact that the government may have formulated, furnished, or in any way supplied the said drawings, specifications, or other data, is not to be regarded by implication or otherwise as in any manner licensing the holder or any other person or corporation, or conveying any rights or permission to manufacture, use, or sell any patented invention that may in any way be related thereto.

This report has been reviewed by the Information Office (IO) and is releasable to the National Technical Information Service (NTIS). At NTIS, it will be available to the general public, including foreign nations.

This technical report has been reviewed and is approved for publication.



TONY G. GERARDI  
Project Engineer

FOR THE COMMANDER



ROBERT M. BADER, Chief  
Structural Integrity Branch  
Structural Mechanics Division

  
Howard L. Farmer

HOWARD L. FARMER, COL, USAF  
Chief, Structural Mechanics Division

Copies of this report should not be returned unless return is required by security considerations, contractual obligations, or notice on a specific document.

UNCLASSIFIED

SECURITY CLASSIFICATION OF THIS PAGE (When Data Entered)

REPORT DOCUMENTATION PAGE		READ INSTRUCTIONS BEFORE COMPLETING FORM
1 AFFILIATION AFFDL-TR-77-37		2 GOVT ACCESSION NO. REF ID: A62740
3 TITLE (and Subtitle) DIGITAL SIMULATION OF FLEXIBLE AIRCRAFT RESPONSE TO SYMMETRICAL AND ASYMMETRICAL RUNWAY ROUGHNESS		4 DATE OF REPORT (month/year) Final Technical Report September 1975 - Aug 1976
5 AUTHOR Ferry G. Gerard Anthony		6 CONTRACT OR GRANT NUMBER Project No. 1367 Task No. 136701 Work Unit No. 13670113
7 PERFORMING ORGANIZATION NAME AND ADDRESS Air Force Flight Dynamics Laboratory Structural Integrity Branch Wright-Patterson AFB, Ohio 45433		8 NUMBER OF PAGES 83
9 CONTROLLING OFFICE NAME AND ADDRESS Air Force Flight Dynamics Laboratory Air Force Systems Command Wright-Patterson AFB, Ohio 45433		10 SECURITY CLASS (if different from block 6) UNCLASSIFIED
11 MONITORING AGENCY NAME & ADDRESS (if different from Controlling Office)		12 DECLASSIFICATION/DOWNGRADING SCHEDULE
13 DISTRIBUTION STATEMENT (of this Report) Approved for public release; distribution unlimited		
14 DISTRIBUTION STATEMENT (of the abstract entered in Block 20, if different from Report)		
15 SUPPLEMENTARY NOTES		
16 KEY WORDS (Continue on reverse side if necessary and identify by block number) Aircraft Dynamics Simulation Ground Loads Taxi Analysis		
17 ABSTRACT (Continue on reverse side if necessary and identify by block number) A method has been developed for determining the dynamic response of a flexible aircraft to runway roughness during takeoff or constant speed taxi. The equations that formulate the mathematical model have been programmed for a CDC 6600 digital computer and uses a Calcomp plotter for part of the program output. Three sets of runway elevation data are input to provide a forcing function at each landing gear. Three runway profiles measured at Washington National Airport, runway 36, were used to represent a typical commercial (OVER)		

DD FORM 1 JAN 73 EDITION OF 1 NOV 6 ...OLETE

UNCLASSIFIED

SECURITY CLASSIFICATION OF THIS PAGE (When Data Entered)

042070

alt

**UNCLASSIFIED**

**SECURITY CLASSIFICATION OF THIS PAGE(When Data Entered)**

Block No. 20 - Continued

asymmetric profile. Three lines of profile were analytically generated to represent traversing a 1-cos dip at a 45 degree angle of approach.

Several aircraft have been simulated with this program, each during a takeoff and a constant speed taxi. The data used to simulate the airplanes (McDonnell Douglas C-9A, Boeing 727-100, and an AMST) and the runway profile data used, are included in the appendix of this paper.

Comparison of simulated results to limited experimental data was good. Peak vertical acceleration levels at the pilot's station were within 14%.

The effect of the asymmetry of a profile on pilot's station vertical acceleration was significant providing the asymmetry of the profile was significant.

**UNCLASSIFIED**

**SECURITY CLASSIFICATION OF THIS PAGE(When Data Entered)**

FOREWORD

This report was prepared by A. G. Gerardi, Aerospace Engineer in the Loads and Response Prediction Group of the Structural Mechanics Division of the Air Force Flight Dynamics Laboratory at Wright-Patterson Air Force Base, Ohio. The work described herein is a part of the Air Force Systems Command exploratory development program to predict aircraft dynamic loads during ground operations. The work was directed under Project 1367, "Structural Integrity for Military Aerospace Vehicles," Task 136701, "Structural Flight Loads Data."

This report covers work done in the period from September 1975 to August 1976.

ACCESSION for	
NTIS	White Section <input checked="" type="checkbox"/>
DDC	Buff Section <input type="checkbox"/>
UNANNOUNCED	<input type="checkbox"/>
JUSTIFICATION _____	
BY _____	
DISTRIBUTION/AVAILABILITY CODES	
Dist. AVAIL AND/or SPECIAL	
A	

## TABLE OF CONTENTS

Section	Page
I    INTRODUCTION	1
1. Purpose of the Study	1
II   MATHEMATICAL MODEL	3
1. General Airplane/Runway Model	3
2. Rigid Body Equations of Motion	6
3. Flexibility Equations of Motion	7
4. Solution Technique	7
III   COMPUTER PROGRAM	9
1. Output Format	9
IV   DISCUSSION OF SIMULATIONS	20
V   SUMMARY AND CONCLUSIONS	38
APPENDIX	
A   DEVELOPMENT OF EQUATIONS OF MOTION	41
B   LISTING OF COMPUTER PROGRAM TAX2	48
C   LISTING OF AIRPLANE DATA	62
D   LISTING OF RUNWAY PROFILE DATA	71
BIBLIOGRAPHY	74
REFERENCES	75

## LIST OF ILLUSTRATIONS

Figure		Page
1.	Accepted Military Human Tolerance Vertical Vibration Criterion	2
2.	Typical Single Acting Oleo Pneumatic Landing Gear Strut	4
3.	Source Deck Setup	16
4.	Typical Calcomp Plotted Output	18
5.	Boeing 727-100 Constant Speed Taxi Simulation over the Washington National Profile Without a Roll Degree of Freedom	22
6.	Boeing 727-100 Constant Speed Taxi Simulation over the Washington National Profile With a Roll Degree of Freedom	23
7.	PSD of Washington National Airport Runway 36	24
8.	Boeing 727-100 Traversing a (1-cos) dip head-on	25
9.	Boeing 727-100 Traversing a (1-cos) dip at a 45° angle	26
10.	C-9A Traversing a (1-cos) dip at a 45° angle	28
11.	AMST Traversing a (1-cos) dip at a 45° angle	29
12.	Boeing 727-100 Taking Off from Washington National Airport With the Roll Degree of Freedom Included	30
13.	AMST Taking Off from Washington National Airport With the Roll Degree of Freedom Included	31
14.	C-9A Taking Off from Washington National Airport With the Roll Degree of Freedom Included	32
15.	PSD of Washington National Runway 36 and two Typically Smooth Runways	33
16.	Measured Response of a Boeing 727-100 Takeoff at Washington National Airport Runway 36	34
17.	C-9A with Flexible Wings Taxiing over a (1-cos) dip at a 45° angle	36

LIST OF ILLUSTRATIONS (Continued)

Figure	Page
18. C-9A with Flexible Wings Taking Off from Washington National Runway 36	37
A-1. Description of Asymmetrical Mathematical Model	42
C-1. Three View of Boeing 727-100	63
C-2. Three View of McDonnell-Douglas C-9A	66
D-1. Washington National Runway 36 with Linear Trend Removed	72

LIST OF TABLES

Table	Page
1 Description of Input Aircraft Data	10
2 Typical Computer Output Listing	17
3 Summary of Simulations	21
Comparisons of Simulated and Experimental Data	35

SECTION I  
INTRODUCTION

A common problem that can occur during takeoff and taxiing operations of aircraft is high acceleration levels caused by a rough runway. Due to these accelerations, runway must be evaluated with respect to roughness in order to ensure timely pavement maintenance to control aircraft structural loads and fatigue. Also, rough runways adversely affect the ability of the crew members by reducing instrument readability and crew comfort. Figure 1 shows the current criterion (Reference 1) used to set maximum allowable vertical acceleration levels from a human comfort standpoint. Reference 2 addressed the runway roughness problem at considerable length and contains the development of a mathematical model and subsequent computer program called "iAXI" to simulate the dynamic response of military aircraft to runway roughness on a symmetrical runway. For a symmetric runway, only one runway profile is required. Normally this is sufficient for representing a paved runway. With the advent of the AMST (Advanced Medium STOL Transport) and in some cases with conventional airplanes operating off of semiprepared or very rough paved surfaces, the rolling motion of an aircraft became significant. This rolling motion was the result of operating the aircraft on an asymmetric runway. Therefore, in order to properly simulate this response it became necessary to include the runway profile encountered by each landing gear.

1. PURPOSE OF THIS STUDY

The purpose of this study is to develop a computer program, capable of simulating an aircraft during constant speed taxi or takeoff from runways that are asymmetric.

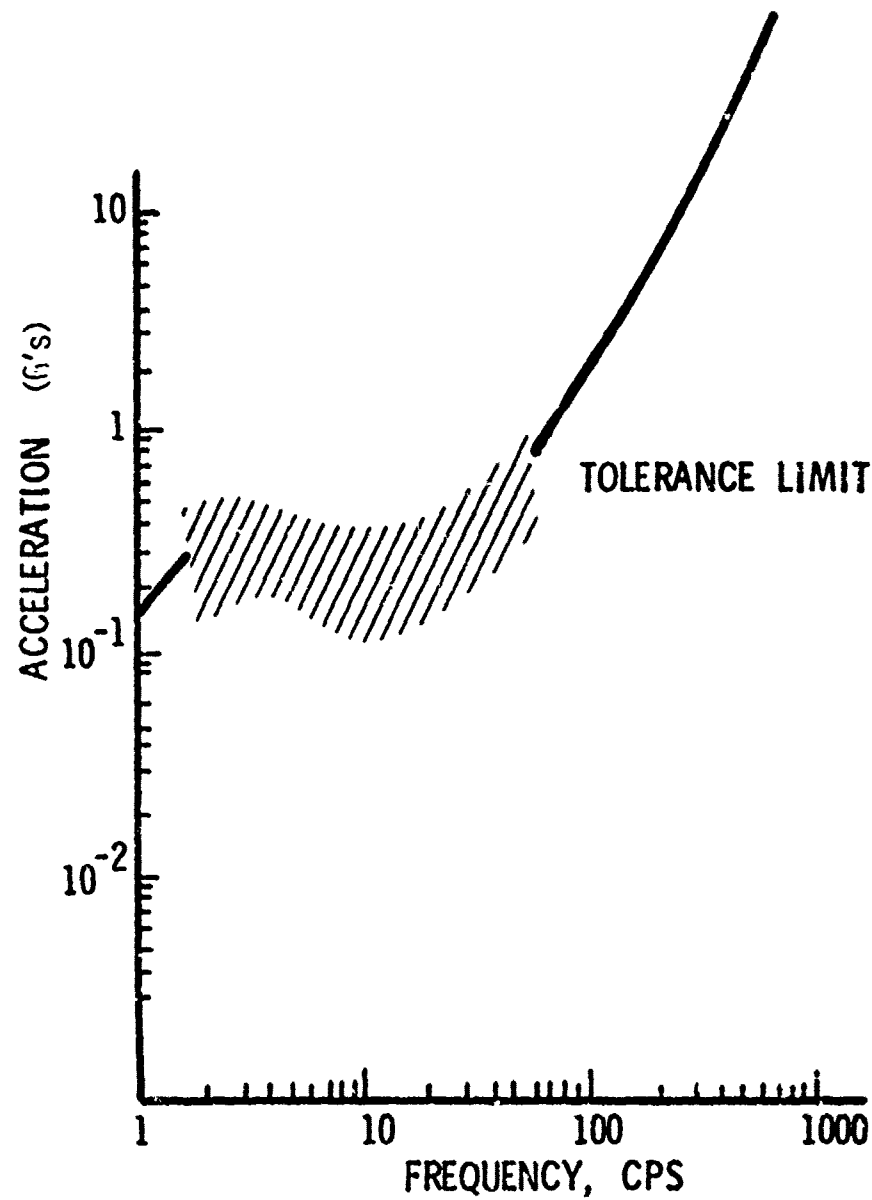


Figure 1. Accepted Military Human Tolerance Vertical Vibration Criterion

## SECTION II MATHEMATICAL MODEL

The airplane/runway mathematical model used for this study was the basic mathematical model developed in Reference 2. A detailed description of the components that make up this general model, as well as the assumptions made are shown in Reference 2. This report presents, in summary form, the landing gear strut and tire representation, the airplane rigid body and flexible body representation, the runway profile representation, the equations of motion, and the solution technique.

### 1. GENERAL AIRPLANE/RUNWAY MODEL

The general model represents an asymmetrical body with a nose gear and a right and left main landing gear. Each landing gear strut is assumed to have point contact with the profile and it is assumed that each landing gear traverses a different profile. Aerodynamic lift and drag are modeled, and thrust is applied at the aircraft's center of gravity.

The airplane is free to roll, pitch, plunge, and translate horizontally down the runway and each landing gear unsprung mass is free to translate vertically. To these rigid body degrees of freedom, up to 30 flexible modes of vibration are included. This airplane motion is controlled by the landing gear strut forces, lift, drag, thrust, and the resisting parameters of aircraft mass and inertia.

The landing gear struts are nonlinear, single acting oleo pneumatic energy absorbing devices (Figure 2) and are represented in the model as the sum of the three forces; pneumatic, hydraulic, and strut bearing friction forces. The pneumatic force, which is the largest of the three is represented by the equation:

$$F_A = \frac{PV}{\frac{V}{A} - S} \quad (1)$$

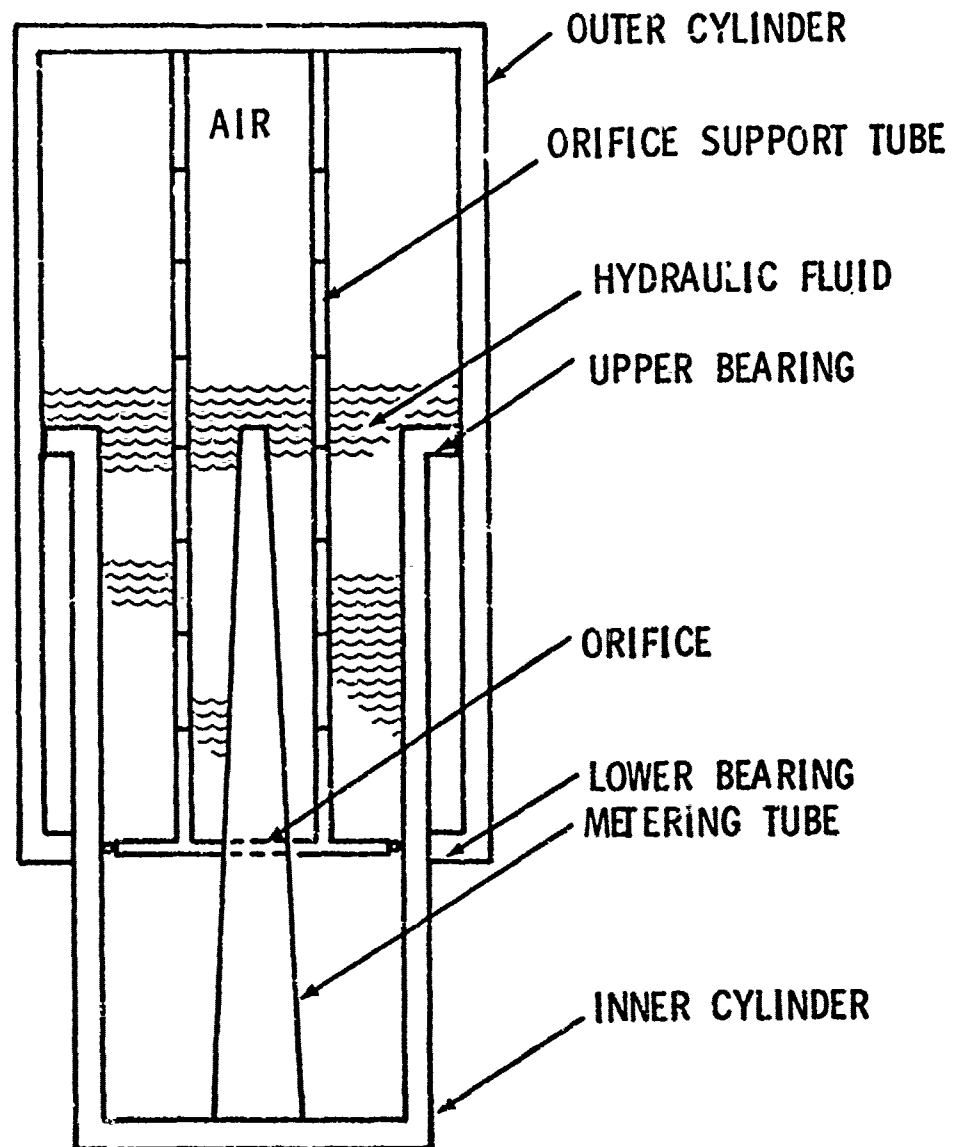


Figure 2. Typical Single Acting Oleo Pneumatic Landing Gear Strut

where:

- P = fully extended strut pressure
- V = fully extended strut volume
- A = pneumatic piston area
- S = strut stroke

The damping force is given by the equation:

$$F_h = \frac{\rho_h A_h^3 \dot{S} |\dot{S}|}{2 (c_d A_o)^2} \quad (2)$$

where:

- $\rho_h$  = density of the hydraulic fluid
- $A_h$  = the hydraulic piston area
- $A_o$  = effective orifice area (constant orifice minus metering pin area)
- $c_d$  = orifice coefficient (use 0.9)
- $\dot{S}$  = strut piston velocity

The third strut force is the strut bearing friction force and is neglected in the model because the force is small for symmetrically loaded struts. (See Reference 2).

The tire force is represented by the linear equation:

$$F_T = k T_D \quad (3)$$

where:

- $T_D$  = tire deflection
- k = linear tire spring constant

The runway elevation data is input into the model in two foot increments. The profile is made continuous by fitting the following

polynomial through the three elevation data points and the slope at the end of the previous profile segment:

$$y(x) = a_1 + a_2x + a_3x^2 + a_4x^3 \quad (4)$$

where:

$a_{1,2,3,4}$  = coefficients derived from the elevation and slope data

This is done for each of the three lines of runway profile data.

## 2. RIGID BODY EQUATIONS OF MOTION

The differential equations of motion for the mathematical model were derived by application of the Lagrange equations (See Appendix A). The general form of these equations is shown below and corresponds to the notation shown in Figure A-1 in Appendix A.

$$\ddot{z} = (F_{s1*} + F_{s2} + F_{s3} + L - W)/M_{cg} \quad [\text{c.g., vertical acceleration}] \quad (5)$$

$$\ddot{z}_1 = (F_{t1} - F_{s1} - W_1)/M_1 \quad [\text{unsprung mass vertical acceleration}] \quad (6)$$

$$\ddot{z}_2 = (F_{t2} - F_{s2} - W_2)/M_2 \quad [\text{unsprung mass vertical acceleration}] \quad (7)$$

$$\ddot{z}_3 = (F_{t3} - F_{s3} - W_3)/M_3 \quad [\text{unsprung mass vertical acceleration}] \quad (8)$$

$$\ddot{\theta} = (F_{s1}A + F_{s2}B + F_{TD}C_1 - F_{s3}C)/I_{yy} \quad [\text{pitching acceleration}] \quad (9)$$

$$\ddot{\phi} = (F_{s3} - F_{s2})C/I_{xx} \quad [\text{rolling acceleration}] \quad (10)$$

$$\ddot{x} = (F_T - F_{TD} - F_{AD})/(M_{cg}) \quad [\text{horizontal translation acceleration}] \quad (11)$$

where:

$F_{s1}, F_{s2}, F_{s3}$  = total landing gear strut forces

$F_{t1}, F_{t2}, F_{t3}$  = tire forces

$M_{cg}$ ,  $W$ ,  $I_{yy}$ ,  $I_{xx}$  = aircraft mass, weight, and pitching and roll inertias

\*The subscript 1, 2 and 3 corresponds to the nose, right main and left main landing gears respectively.

$w_1, w_2, w_3$  = unsprung landing gear weights  
 $A, B, C, \epsilon_1$  = moment arms  
 $L, F_T, F_{TD}, F_{AD}$  = lift, thrust, and tire and aerodynamic drag forces  
[ $F_T$  and  $F_{AD}$  act through the center of gravity]

### 3. FLEXIBILITY EQUATIONS OF MOTION

$$\ddot{M_i q_i} = \epsilon_{i1} F_{s1} + \epsilon_{i2} F_{s2} + \epsilon_{i3} F_{s3} - 2\zeta_i \omega_i \dot{q}_i - \omega_i^2 M_i q_i \text{ for the } i\text{th mode}$$

where:

$M_i$  = the generalized mass  
 $\epsilon_{i1}, \epsilon_{i2}, \epsilon_{i3}$  = modal deflections at gear location 1, 2 and 3  
 $\omega_i$  = modal frequency  
 $\zeta$  = damping factor  
 $q_i = \dot{q}_i, \ddot{q}_i$  = generalized coordinates and their time derivatives.

The sign convention is as follows:

$Z$ = Vertical Displacement	+ up
$\theta$ = Pitch	+ nose down
$\phi$ = Roll	+ roll right
$q$ = Deflection Due to Bending	+ up
$X$ = Horizontal Translation	+ forward

### 4. SOLUTION TECHNIQUE

The technique used for solving the coupled nonlinear differential equations of motion that describe the simulated aircraft is a three-term Taylor series. For example, the equation:

$$\ddot{x} = -cx' - kx \quad (12)$$

The three term Taylor series representations can be written as

$$x_{(I+1)} = x_{(I)} + \dot{x}_{(I)} (\Delta t) + \ddot{x}_{(I)} \frac{(\Delta t)^2}{2} \quad (13)$$

where:  $I = 1 \rightarrow N$

The values for  $\ddot{x}$ ,  $\dot{x}$  and  $x$  from the previous step are substituted into Equation 13 and a new value for  $x$  is obtained. Differentiating Equation 13 we obtain for the velocity  $\dot{x}$ , the expression:

$$\dot{x}_{(I+1)} = \dot{x}_{(I)} + \ddot{x}_{(I)} (\Delta t) \quad (14)$$

The values for  $\dot{x}$  and  $\ddot{x}$  are then substituted into Equation 14 and a new value of  $\dot{x}$  is found. This entire process is repeated with the new values of  $x$  and  $\dot{x}$  to obtain the next point in the solution.

### SECTION III COMPUTER PROGRAM

The computer program, TAX2, which computes the dynamic response of a flexible aircraft to an asymmetrical runway profile, consists of one basic program and several subroutines. A complete listing of the program is contained in Appendix B. Table 1 contains a description of the aircraft input data and Figure 3 shows the source deck setup for use on the CDC 6600 computer at Wright-Patterson AFB, Ohio.

#### 1. OUTPUT FORMAT

The results of the calculations are presented as both a printed output and a time history plot. The printed output lists the value of fifteen parameters each 0.01 second. A sample of this listed output is shown in Table 2. The fifteen parameters listed in the heading are:

XMAINL	- Left Main landing gear strut deflection (inches)
XMAINR	- Right Main landing gear strut deflection (inches)
XNOSE	- Nose gear strut deflection (inches)
ZPML	- Left Main landing gear runway elevation (inches)
ZPMR	- Right Main landing gear runway elevation (inches)
ZPN	- Nose landing gear runway elevation (inches)
BETADD	- Rolling acceleration ( $\dot{\phi}$ ) (rad/sec $^2$ )
THETADD	- Pitching acceleration ( $\ddot{\theta}$ ) (rad/sec $^2$ )
BETA	- Roll angle ( $\phi$ ) (rad)
THETA	- Pitch angle ( $\theta$ ) (rad)
SPEED	- Aircraft velocity (ft/sec)
DISTANCE	- Distance traveled down the runway (feet)
TIME	- Real time (seconds)
CGACC	- Center of Gravity Vertical Acceleration (g's)
PSA	- Pilot's Station Vertical Acceleration (g's)

Figure 4 shows a photographic reduction of a typical Calcomp-plotted time history. This figure depicts a Boeing 727-100 taxiing at 50 fps over a 1-cos bump at a 45° angle of approach. The plotted output includes titles showing the airplane simulated, its gross weight,

TABLE 1  
DESCRIPTION OF INPUT AIRCRAFT DATA

Section 1 (cards 1-5) - General Airplane Data

Card Column	Format	Variable Name	Data for McDonnell-Douglas C-9A	Definition
<u>Card 1</u>				
1-80	8A10	PLANE	McDonnell-Douglas C-9A	Airplane Being Simulated and Gross Weight
<u>Card 2</u>				
1-10	F10.1	W	108000.	Vehicle Weight (lbs)
11-20	F10.1	A	51.6	Distance Main Gear to CG (in)
21-30	F10.1	B	589.4	Distance Nose Gear to CG (in)
31-40	F10.1	MMI	20800000.	Pitch Moment of Inertia (lb in sec <sup>2</sup> )
41-52	F12.0	WS	96.	Wing Station of Main Gear (in)
53-64	F12.0	MMIR	8000000.	Roll Moment of Inertia (lb in sec <sup>2</sup> )
<u>Card 3</u>				
1-10	F10.2	PSARM	607.0	Distance of Pilot Station to CG (in)
11-20	F10.2	TAILRM	318.5	Distance of Tail Station to CG (in)
<u>Card 4</u>				
1-10	F10.2	SPEED	50.	Initial Velocity of Airplane (ft/sec)
11-20	F10.2	THRUST	29000.	Total Airplane Thrust (lbs)
21-30	F10.2	TAKOFF	285.5	Airplane Rotation Speed (ft/sec)

TABLE 1 (Continued)

Card Column	Format	Variable Name	Data for McDonnell- Douglas C-9A	Definition
<u>Card 5</u>				
1-10	F10.4	CL	1.1	Lift Coefficient
11-20	F10.4	AREA	1000.7	Wing Area ( $\text{ft}^2$ )
21-30	F10.4	CD	.1	Drag Coefficient
<u>Section 2 (cards 6-11) - Main and Nose Gear</u>				
<u>Card 6</u>				
1-10	F10.2	WM	957.16	Unsprung Weight of Each Main Gear (lbs)
11-20	F10.2	WN	153.43	Unsprung Weight of Nose Gear (lbs)
21-30	F10.2	SXM	2.	Number of Main Gear Struts
31-40	F10.2	SXN	1.	Number of Nose Gear Struts
<u>Card 7</u>				
1-10	F10.5	AHN	6.745	Hydraulic Piston Area Nose ( $\text{in}^2$ )
11-20	F10.5	AAN	8.2958	Pneumatic Piston Area Nose ( $\text{in}^2$ )
21-30	F10.5	AHM	16.5	Hydraulic Piston Area Main ( $\text{in}^2$ )
31-40	F10.5	AAM	21.648	Pneumatic Piston Area Main ( $\text{in}^2$ )
<u>Card 8</u>				
1-10	F10.5	PAOH	120.	Nose Strut Preload Pressure (lbs/ $\text{in}^2$ )
11-20	F10.5	PAOM	220.	Main Strut Preload Pressure (lbs/ $\text{in}^2$ )

TABLE I (Continued)

Card Column	Format	Variable Name	Data for McDonnell- Douglas C-9A	Definition
21-30	F10.5	VON	126.2	Fully Extended Nose Strut Air Volume (in <sup>3</sup> )
31-40	F10.5	VOM	366.0	Fully Extended Main Strut Air Volume (in <sup>3</sup> )
41-50	F10.5	OAM	.543	Orifice Area Main (in <sup>2</sup> )
51-60	F10.5	OAN	.442	Orifice Area Nose (in <sup>2</sup> )
<u>Card 9</u>				
1-10	F10.3	SLM	85.5	Distance from Axle to CG Waterline Main Gear Strut Unloaded (in)
11-20	F10.3	SLN	87.3	Distance from Axle to CG Waterline Nose Gear Strut Unloaded (in)
<u>Card 10</u>				
1-10	F10.1	TSM	23428.6	Main Tire Spring Constant Per Strut (lbs/in)
11-20	F10.1	TSN	8632.5	Nose Tire Spring Constant Per Strut (lbs/in)
<u>Card 11</u>				
1-10	F10.5	DX	.001	Integration Step Size
<u>Card 12</u>				
1-5	I5	IFPLOT	0	0-Plot; 1-No Plot
6-10	I5	IFLIST	0	0-List; 1-No List
<u>Section 3 (cards 13-16) - Metering Pin Description</u>				
<u>Card 13</u>				
1-5	I5	NSCN	5	Number of Slope Changes Nose Gear

TABLE 1 (Continued)

Card Column	Format	Variable Name	Data for McDonnell-Douglas C-9A	Definition
<u>* Card 14A, 14B,....</u>				
1-10	F10.3	STROKN (1)	*	Stroke Corresponding to Metering Pin Diameter, Nose Gear
11-20	F10.3	PINDN (1)	*	Metering Pin Diameter, Nose Gear (in)
<u>Card 15</u>				
1-5	I5	NSCM	*	Number of Slope Changes Main Gear
<u>* Card 16A, 16B,....</u>				
1-10	F10.3	STROKM (1)	*	Stroke Corresponding to Metering Pin Diameter, Nose Gear
11-20	F10.3	PINDM (1)	*	Metering Pin Diameter, Main Gear (in)
<u>Section 4 (cards 17-19) - Flexibility Data</u>				
<u>Card 17</u>				
1-5	I5	NFM	7	Number of Symmetrical Flexible Modes
6-10	I5	NAFM	7	Number of Asymmetrical Modes
<u>** Card 18A, 18B,....</u>				
1-10	F10.3	SIMAIN (1)	**	Mode Shape Deflection Main Gear
11-20	F10.3	SINOSE (1)	**	Mode Shape Deflection Nose Gear
21-30	F10.3	SICG (1)	**	Mode Shape Deflection CG
31-40	F10.3	SITAIL (1)	**	Mode Shape Deflection Tail Station

TABLE 1 (Continued)

Card Column	Format	Variable Name	Data for McDonnell- Douglas C-9A	Definition
41-50	F10.3	SIPS	**	Mode Shape Deflection Pilot Station
<u>** Card 19A, 19B,....</u>				
1-15	F15.2	GM (I)	**	Generalized Mass ( $\text{lbs sec}^2/\text{in}$ )
<u>** Card 20A, 20B,....</u>				
1-10	F10.3	SILEFT (I)	**	Deflection for Left Main Gear
11-20	F10.3	SIRIGHT (I)	**	Deflection for Right Main Gear
<u>** Card 21A, 21AB,....</u>				
1-15	F15.3	GMA (I)	**	Asymmetrical Generalized Mass ( $\text{lbs sec}^2/\text{in}$ )
16-25	F10.4	OMEGA (I)	**	Asymmetrical Modal Frequency (rad/sec)

\* One card is required for each stroke-metering pin combination read into the program.

\*\* One card is required for each flexible mode.

Note: A summary of all the data used in this study is shown in Appendix C.

TABLE 1 (Concluded)

Runway Profile Magnetic Tape

The runway profile is read into the program from a magnetic tape or permanent file. The format for this is shown below:

Column	Format	Variable Name	Definition
<u>Read 1</u>			
1-80	8A10	SITE**	Runway Profile and Direction
<u>Read 2</u>			
1-6	I6	NPTSS**	Number of Runway Elevation Points
<u>* Read 3, 4,...,N+2</u>			
1-70	10F7.3	ELEV**	Runway Profile Data
		ELEV	
		ELEVR	

---

\* One read required for every ten runway profile elevation points.

\*\* The process is repeated for each of the three profiles.

Note: All of the runway profile data used in this study is listed in Appendix D.

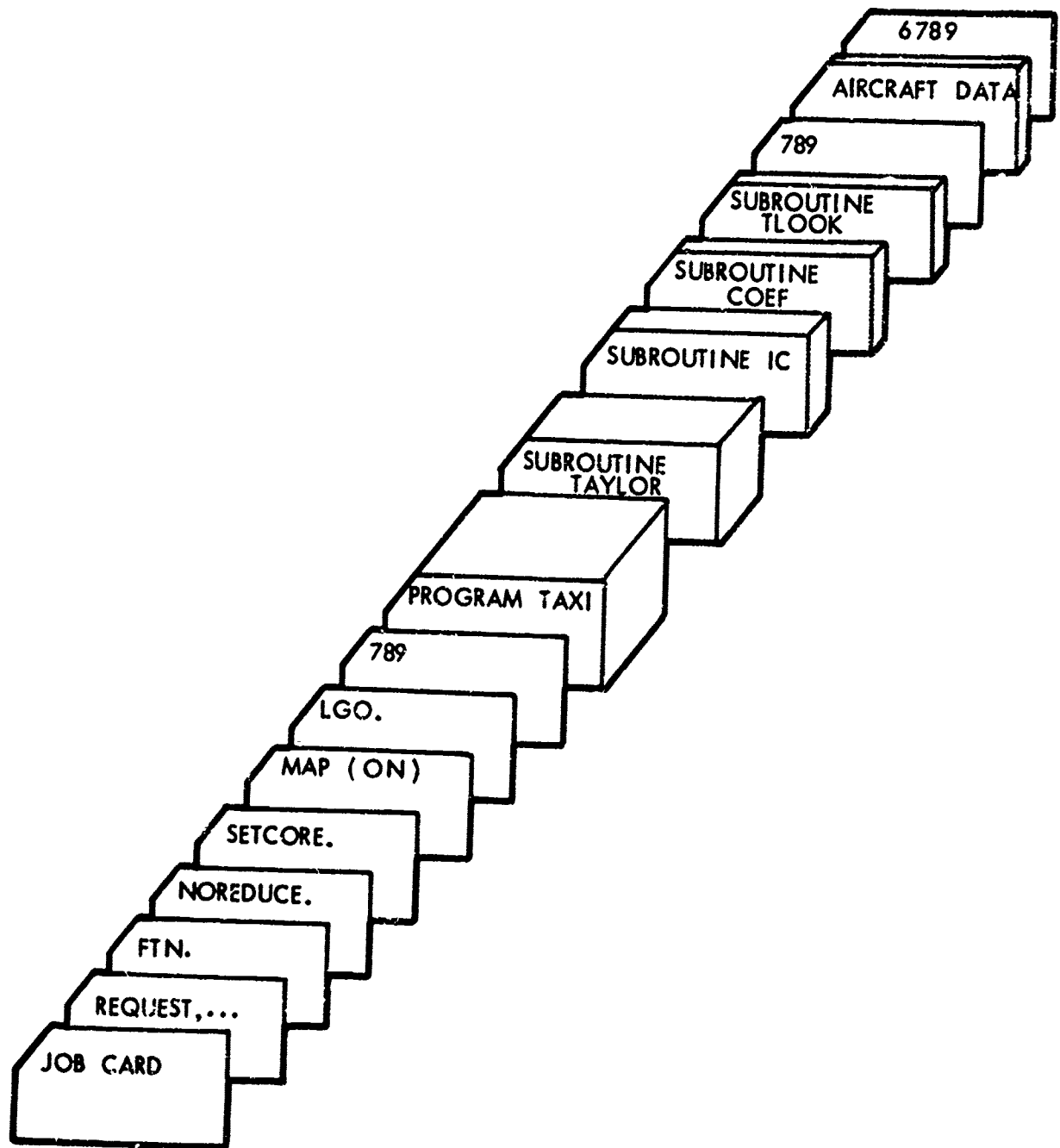


Figure 3. Source Deck Setup

**BEST AVAILABLE COPY**

TABLE 2  
TYPICAL COMPUTER OUTPUT LISTING

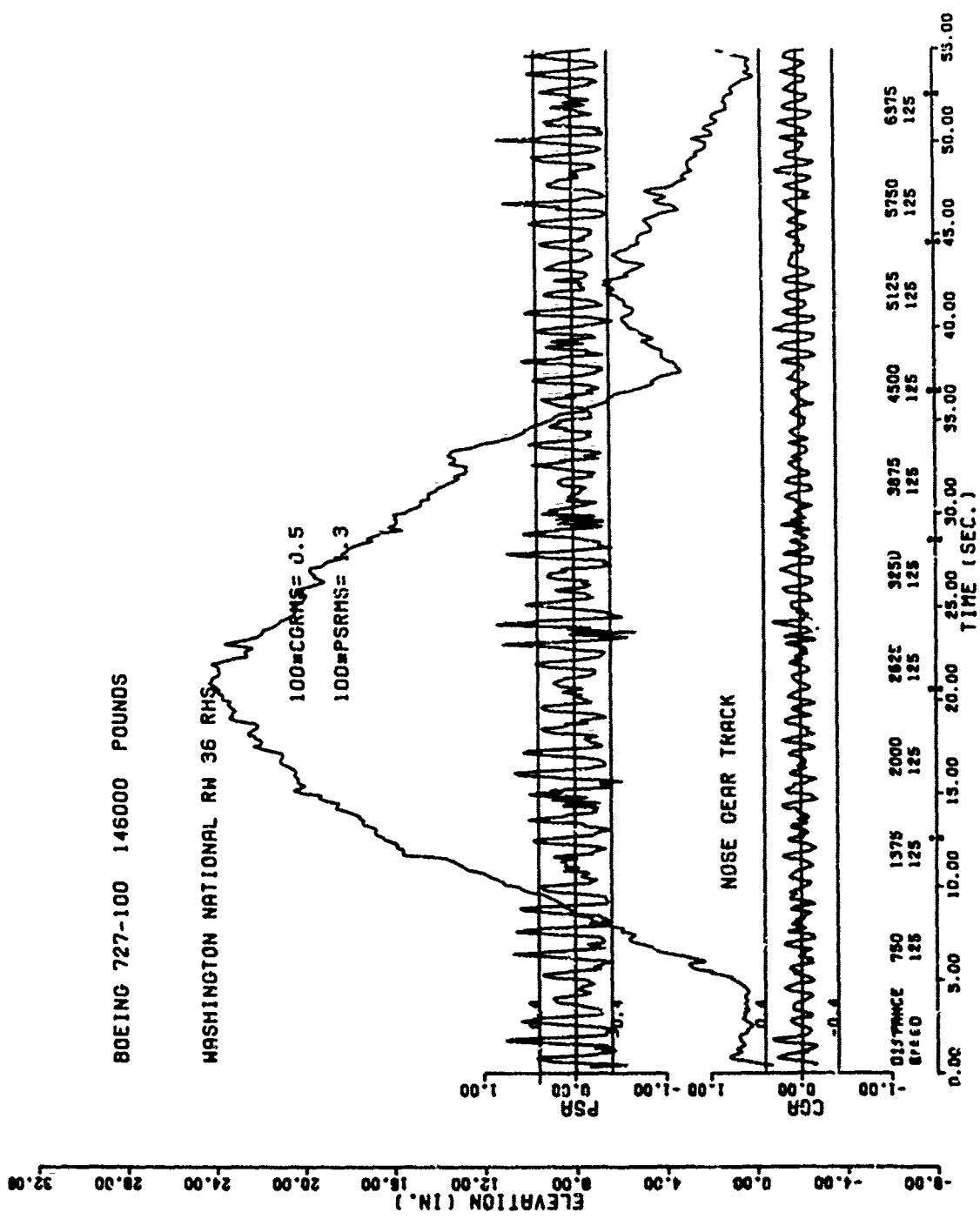


Figure 4. Typical Galcomp Plotted Output

the runway number and its location. The abscissa is the time axis annotated every second. At every time annotation the current value of aircraft speed, in feet per second, and the current aircraft position on the runway, in feet, are printed out. Runway markers (1,000-foot markers) are also plotted on the time scale to aid in aircraft positioning. The plot titled "Nose Gear Track" is a time history of the runway profile as it is encountered by the aircraft's nose gear. The actual runway profile is preceded by 100 feet of smooth surface to allow any starting transients to damp out prior to encountering the actual profile. There are two aircraft acceleration time histories that are of particular interest. One is the vertical acceleration at the pilot's station (PSA), the other is the vertical acceleration at the aircraft's center of gravity (CGA). Each time history is banded by the human tolerance criterion of  $\pm 0.4$  g. In order to minimize the amount of computer central memory required to store the acceleration time histories, the higher frequency components were effectively filtered out by limiting the sampling interval. All of the acceleration peaks, however, are shown on the plot. It should be noted that the pilot station acceleration time history is not always within the band of accepted human tolerance criteria. Thus, the plot is very useful in that it provides a graphical record of the level of acceleration, and it shows which bumps in the runway profile caused the high acceleration response.

## SECTION IV DISCUSSION OF SIMULATIONS

Table 3 contains a summary of the simulations made in this study. Three different airplanes were simulated: the Boeing 727-100, the McDonnell Douglas C-9A, and an AMST configuration. Each airplane was simulated traversing two profiles: Washington National Runway 36, and a 1-cos dip. Simulations were made using mathematical models with and without a roll degree of freedom, i.e. one or three profiles, and with and without flexible wings so that comparisons of the responses could be made.

Figures 5 and 6 show the plotted results of a Boeing 727-100 traversing the Washington National runway profile without a roll degree of freedom and with a roll degree of freedom respectively. Both runs were made at a constant speed of 125 feet per second, because this speed produced higher levels of vertical acceleration for this airplane. Comparison of these two figures shows a significant increase in the vertical acceleration at the pilot's station (P.S.) while the aircraft is at different locations on the runway. For example, at T=46 sec. P.S. acceleration levels more than doubled when three lines of profile were used. This is attributed to the fact that the profiles seen by the main landing gear were rougher in the latter case. Figure 7 shows the Power Spectral Density (PSD) levels of each line of survey for the Washington National runway. A PSD is a measure of the relative roughness of a runway versus frequency. It can be seen, that the PSD level is different for each line of survey which accounts for the change in the aircraft's dynamic response. Figures 8 and 9 show the 727-100 traversing a 1-cos dip headon and at a 45° angle respectively. In this case the speed was 50 fps which "tunes" the natural pitching frequency (1 cps) of the 727-100 to this 1-cos dip. Hitting the 1-cos dip at an angle caused an increase in the peak P.S. and C.G. acceleration levels.

It was necessary to try to simulate different aircraft with the computer program in an effort to check the program's versatility.

TABLE 3  
SUMMARY OF SIMULATIONS

Run #	Airplane	Profile	Speed	Remarks
1	727-100	Washington National (C)	125 fps	No Roll DOF*, Rigid Wings
2	727-100	Washington National (L,C,R)	125 fps	With Roll DOF, Rigid Wings
3	727-100	(1-cos) (C)	50 fps	No Roll DOF, Rigid Wings
4	727-100	(1-cos) (L,C,R)	50 fps	With Roll DOF, Rigid Wings
5	C-9A	(1-cos) (L,C,R)	50 fps	With Roll DOF, Rigid Wings
6	AMST	(1-cos) (L,C,R)	50 fps	With Roll DOF, Rigid Wings
7	727-100	Washington National (L,C,R)	Takeoff	With Roll DOF, Rigid Wings
8	AMST	Washington National (L,C,R)	Takeoff	With Roll DOF, Rigid Wings
9	C-9A	Washington National (L,C,R)	Takeoff	With Roll DOF, Rigid Wings
10	C-9A	(1-cos) (L,C,R)	50 fps	With Roll DOF, Flexible Wings
11	C-9A	Washington National (L,C,R)	Takeoff	With Roll DOF, Flexible Wings

\* Degree of Freedom

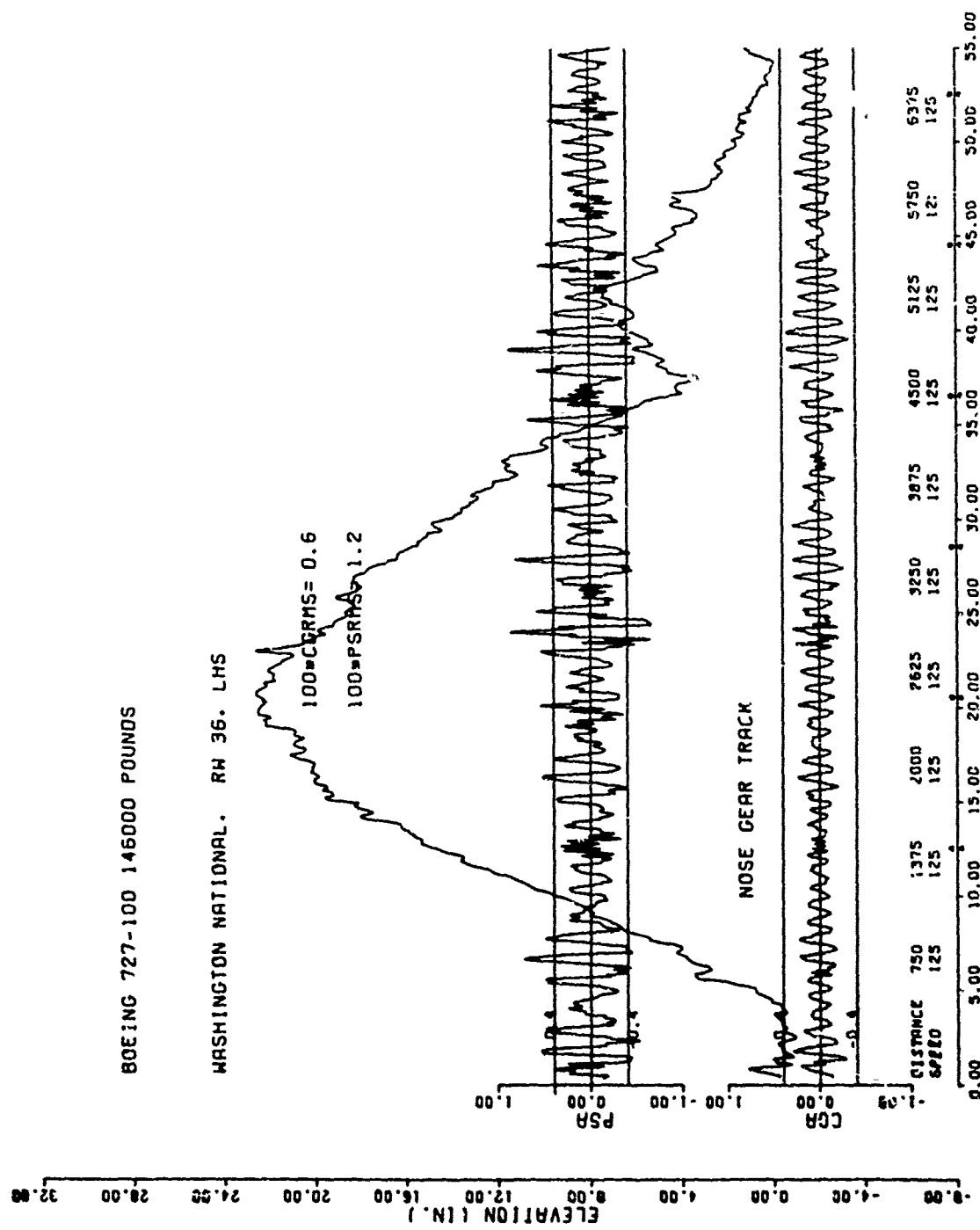


Figure 5. Boeing 727-100 Constant Speed Taxi Simulation over the Washington National Profile Without a Roll Degree of Freedom

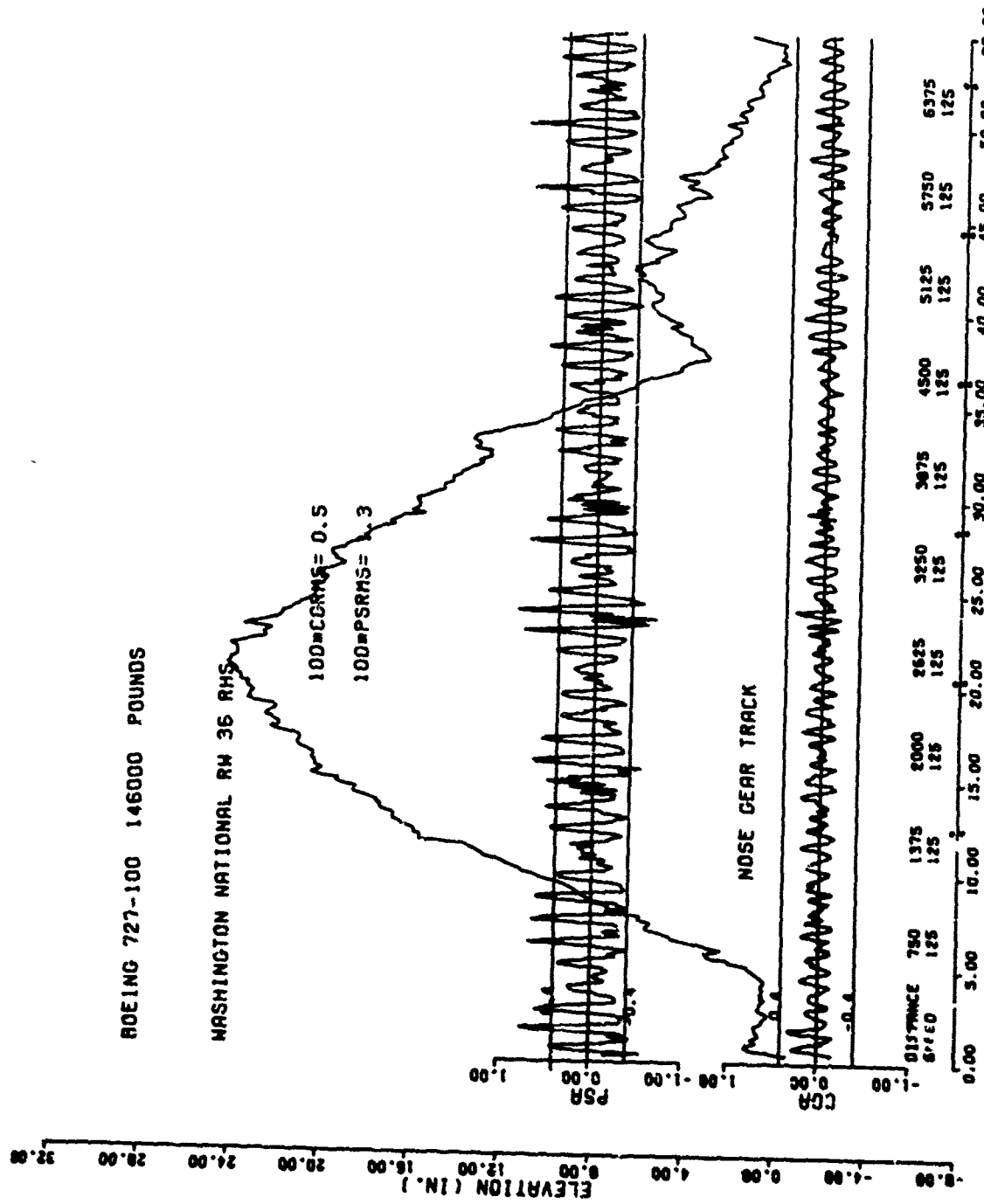


Figure 6. Boeing 727-100 Constant Speed Taxi Simulation over the Washington National Profile With a Roll Degree of Freedom

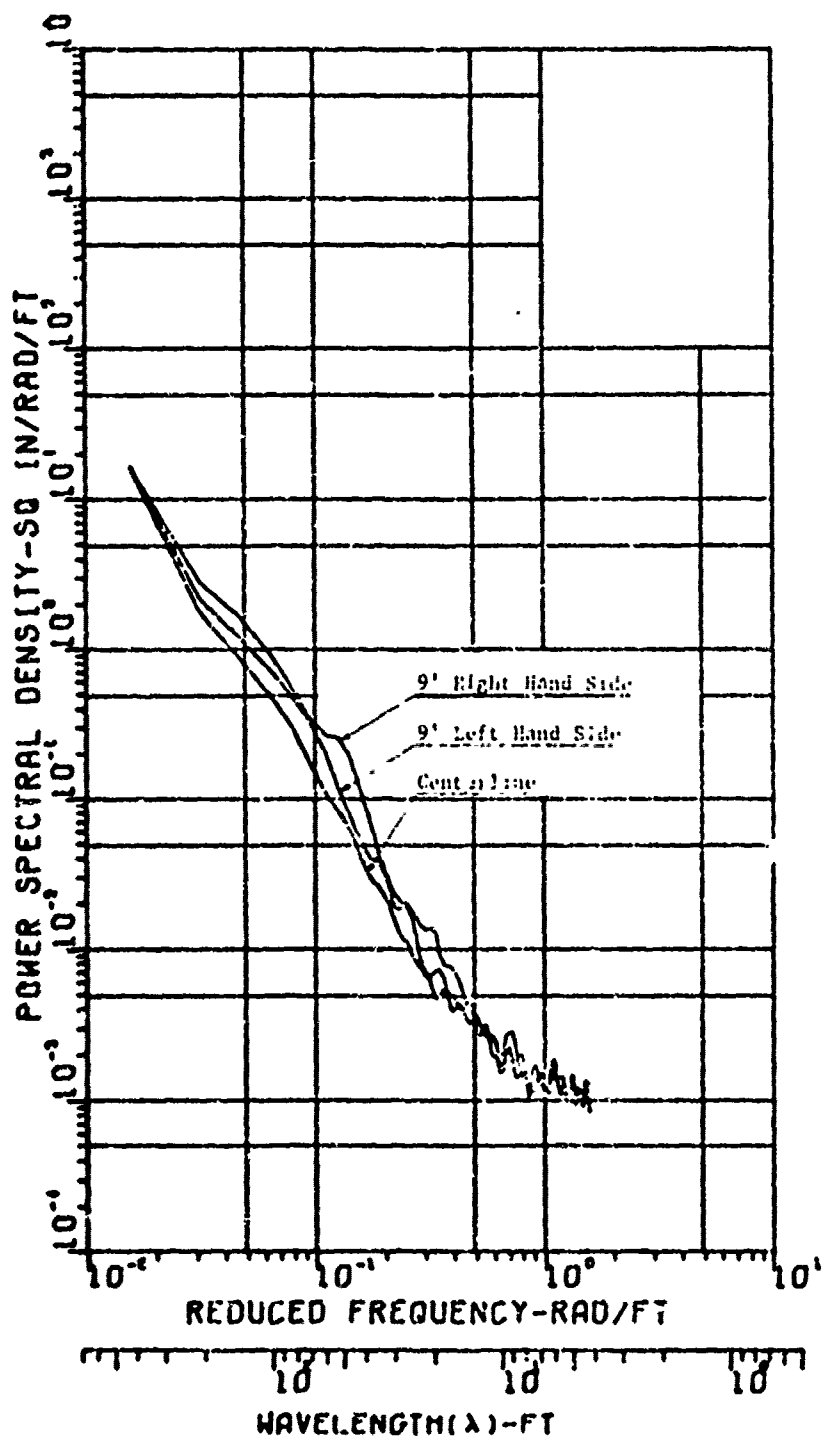


Figure 7. PSD of Washington National Airport Runway 36

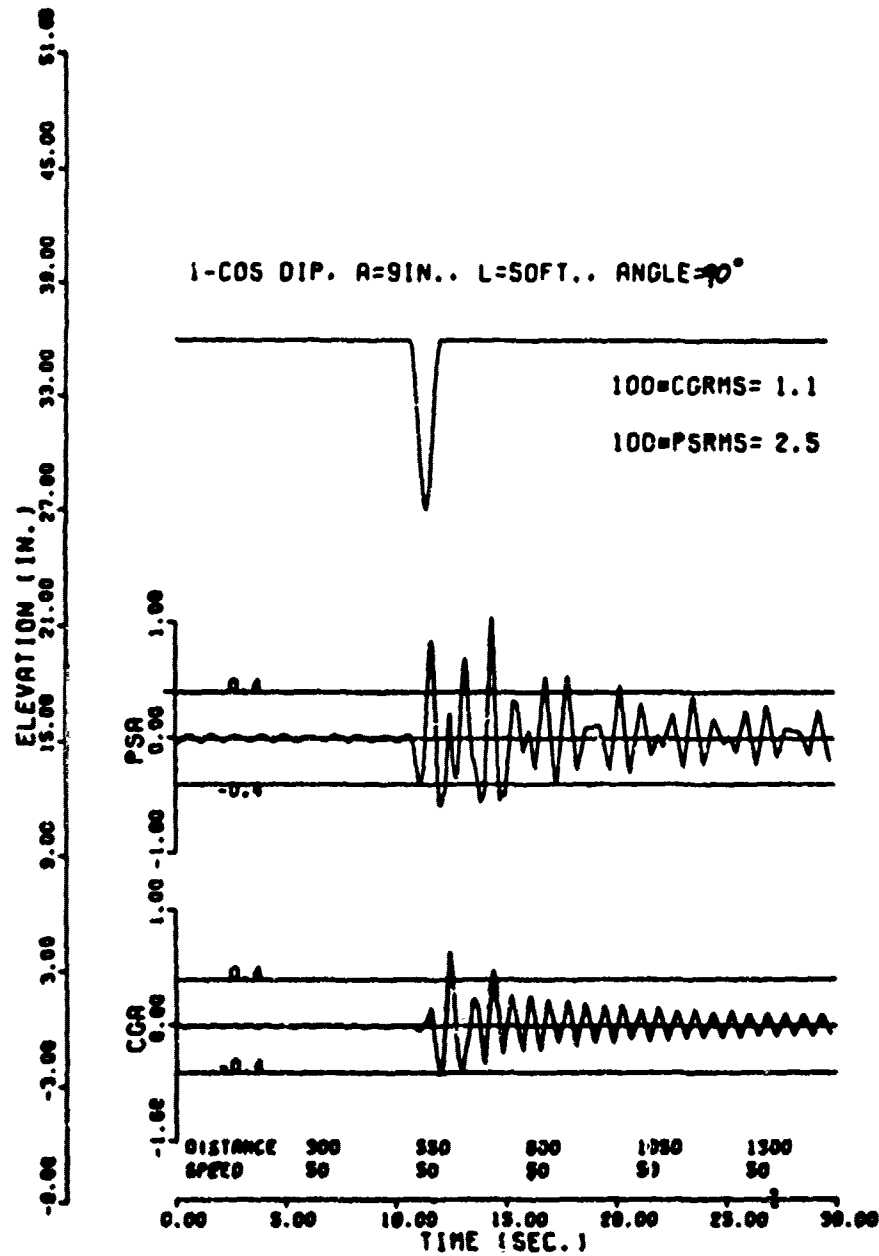


Figure 8. Boeing 727-100 Traversing a (1-cos) dip head-on.

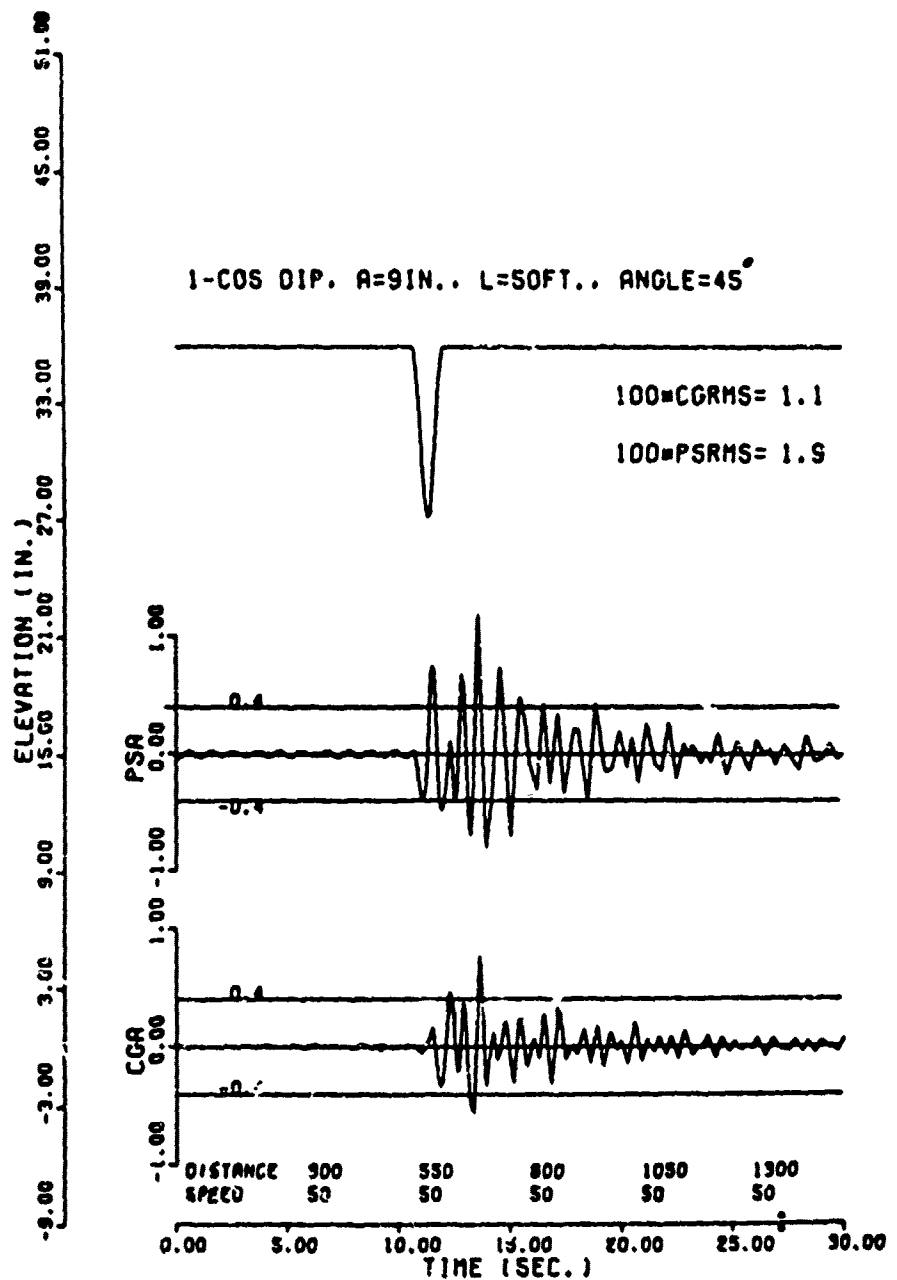


Figure 9. Boeing 727-100 Traversing a (1-cos) dip at a 45° angle

Figures 10 and 11 show the plotted results of the C-9A and AMST respectively hitting the 1-cos dip at a 45° angle at a constant speed of 50 fps. While the C-9A had a relatively high response, the AMST, which is designed to operate off of rough fields, "absorbed" the dip to a large degree. This indicates that the computer program is calculating relative responses which are at least intuitively correct.

Up to this point only constant speed simulations have been discussed. Figures 12, 13 and 14 show the plotted results of the Boeing 727-100, AMST and the C-9A respectively taking off from the Washington National runway profile. Takeoff simulations are made by starting at a near zero forward velocity and accelerating at a constant thrust until rotation speed is reached, then the simulation is terminated. Again it can be seen that the AMST (which is designed for rough field operation) had a very low dynamic response, even though this runway is relatively rough. Figure 15 shows the plotted PSD's of Washington National Runway 36 and of two typically smooth runways, one at Portland Oregon and one at Dulles International. The Washington National Runway is significantly rougher.

Experimental data was available for comparison with the 727-100 takeoff simulation. Figure 16 shows the actual time history plots of vertical acceleration measured on a 727-100 taking off at 120,000 pounds gross weight from Washington National Runway 36 on December 11, 1972. Some parameters of the test aircraft were unknown such as strut and tire pressures and actual inertias. So exact simulation was not possible. However, Table 4 shows that comparison of several peak values of vertical accelerations at the P.S. were within 15 percent. The comparisons of C.G. vertical accelerations were not as good. In the simulation the acceleration levels were lower. It appears that main gear strut pressures on the actual airplane were lower than that simulated. This difference would cause the higher response in the plunge mode.

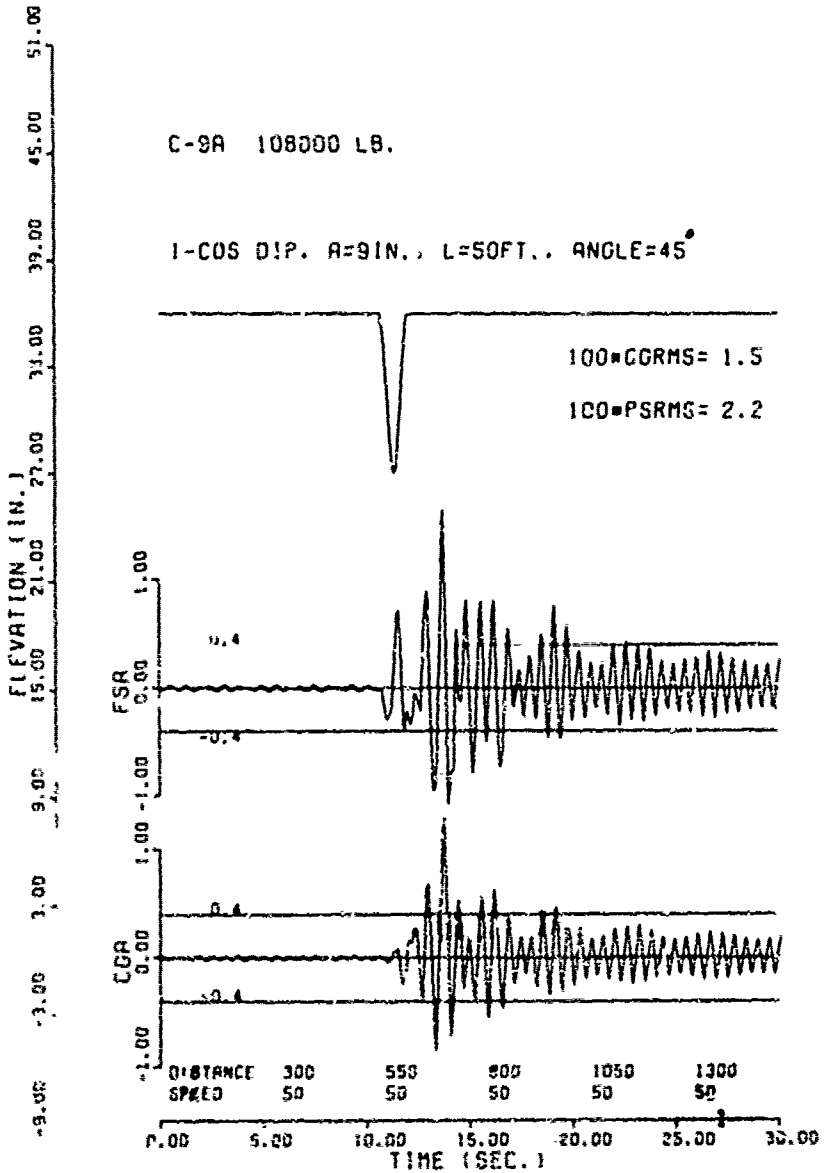


Figure 10. C-9A Traversing a ( $i$ -cos) dip at a  $45^\circ$  angle

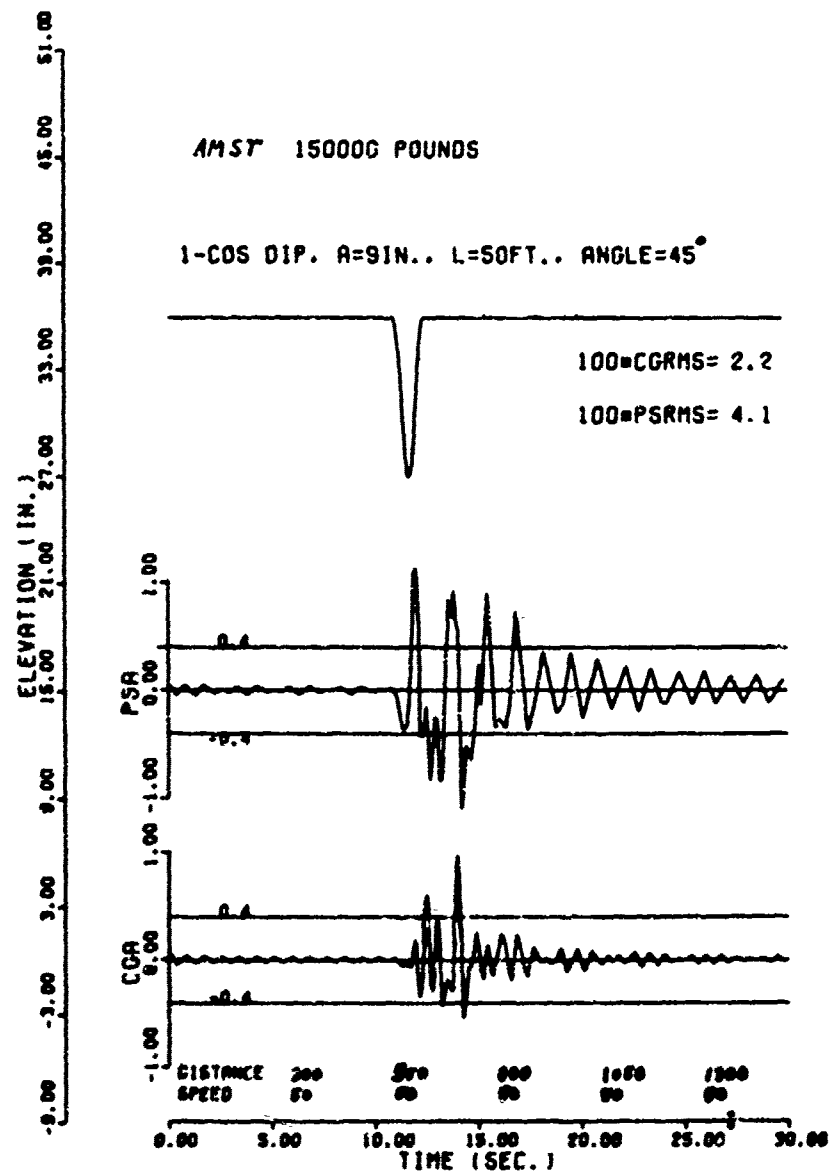


Figure 11. AMST Traversing a (1-cos) dip at a 45° angle

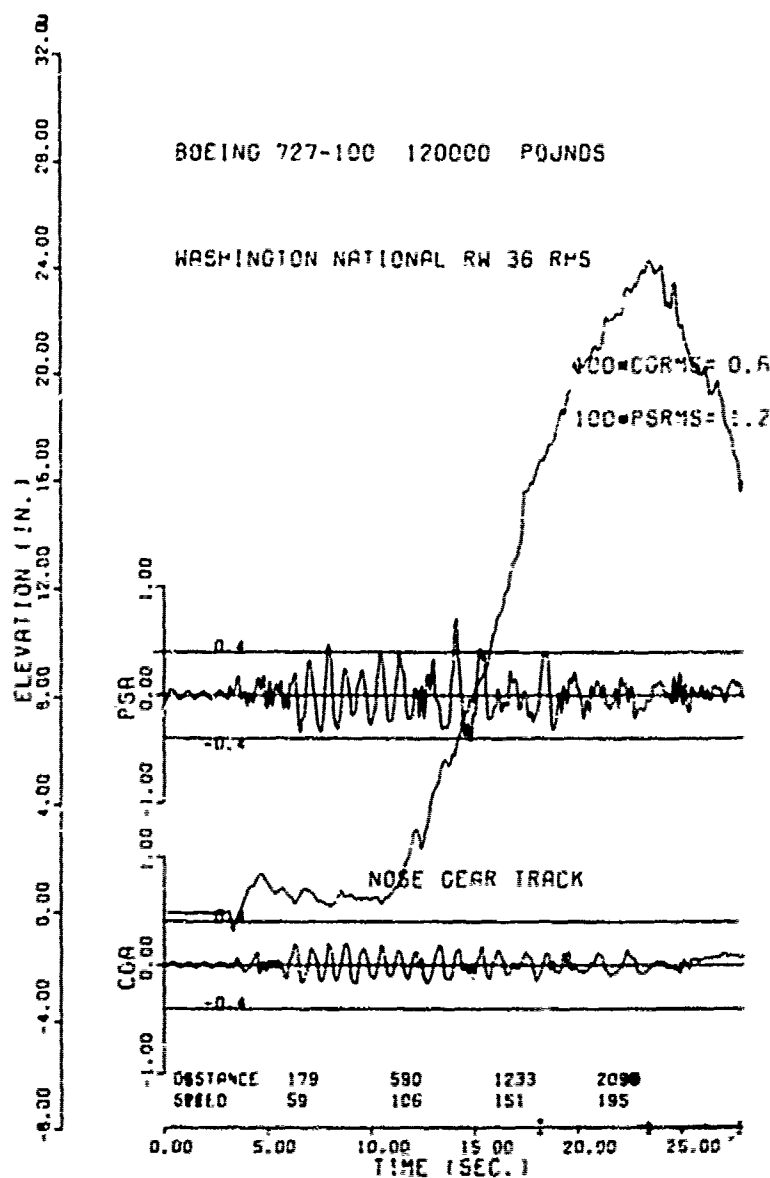


Figure 12. Boeing 727-100 Taking Off from Washington National Airport With the Roll Degree of Freedom Included

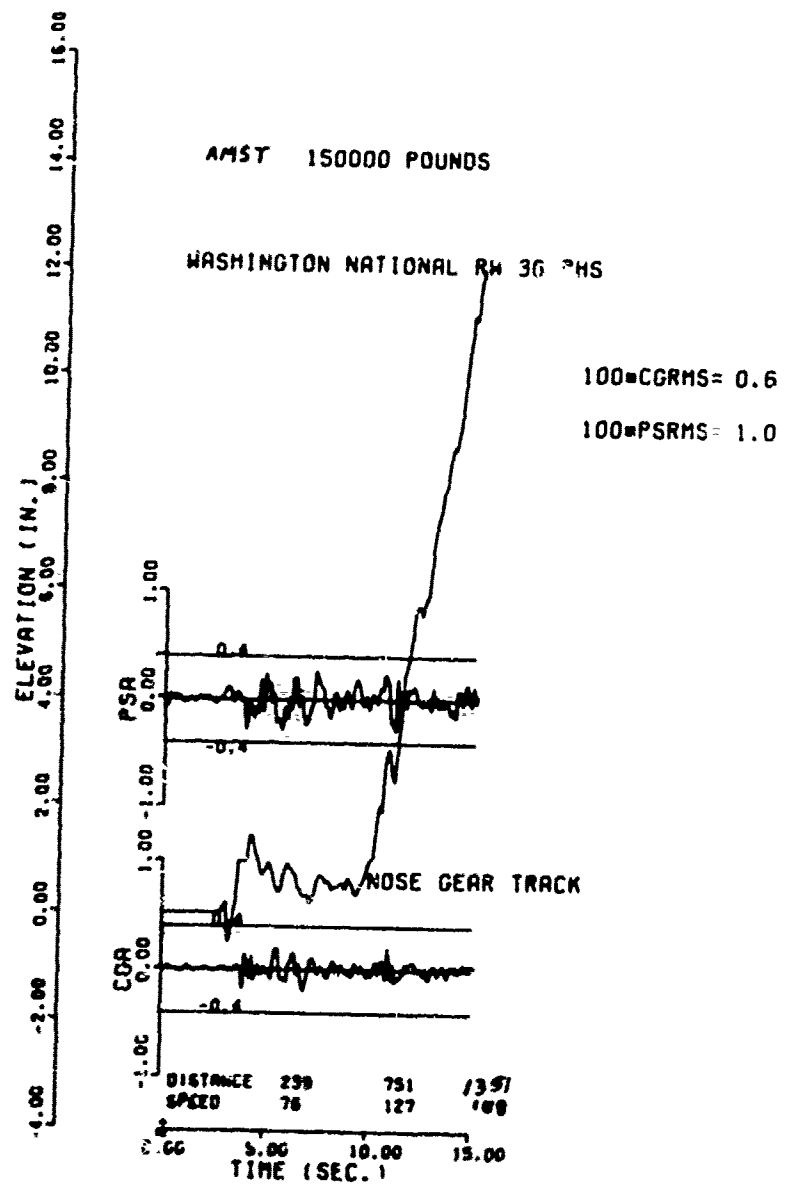


Figure 13. AMST Taking Off from Washington National Airport With the Roll Degree of Freedom Included

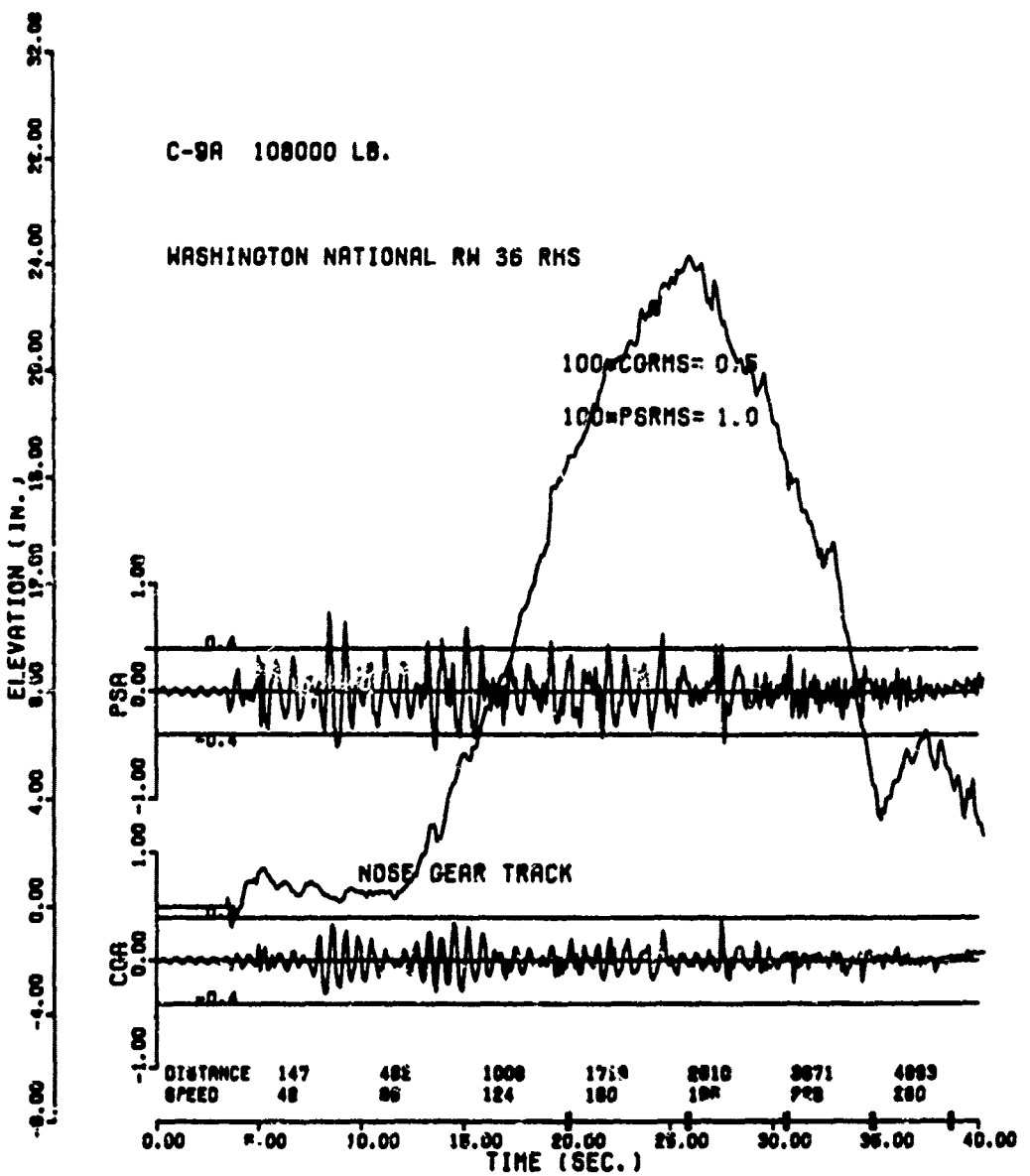


Figure 14. C-9A Taking Off from Washington National Airport With the Roll Degree of Freedom Included

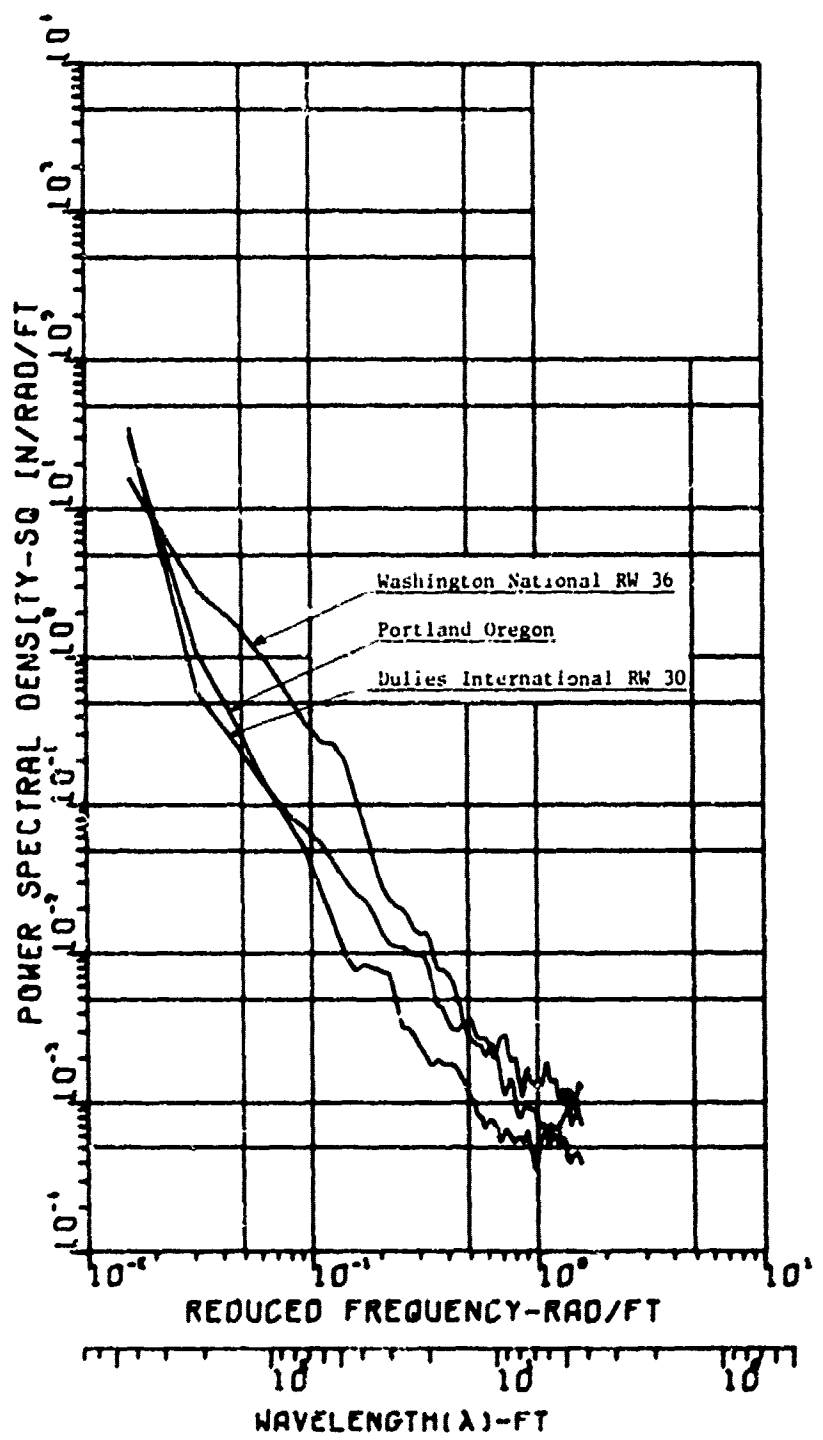


Figure 15. PSD of Washington National Runway 36 and two Typically Smooth Runways

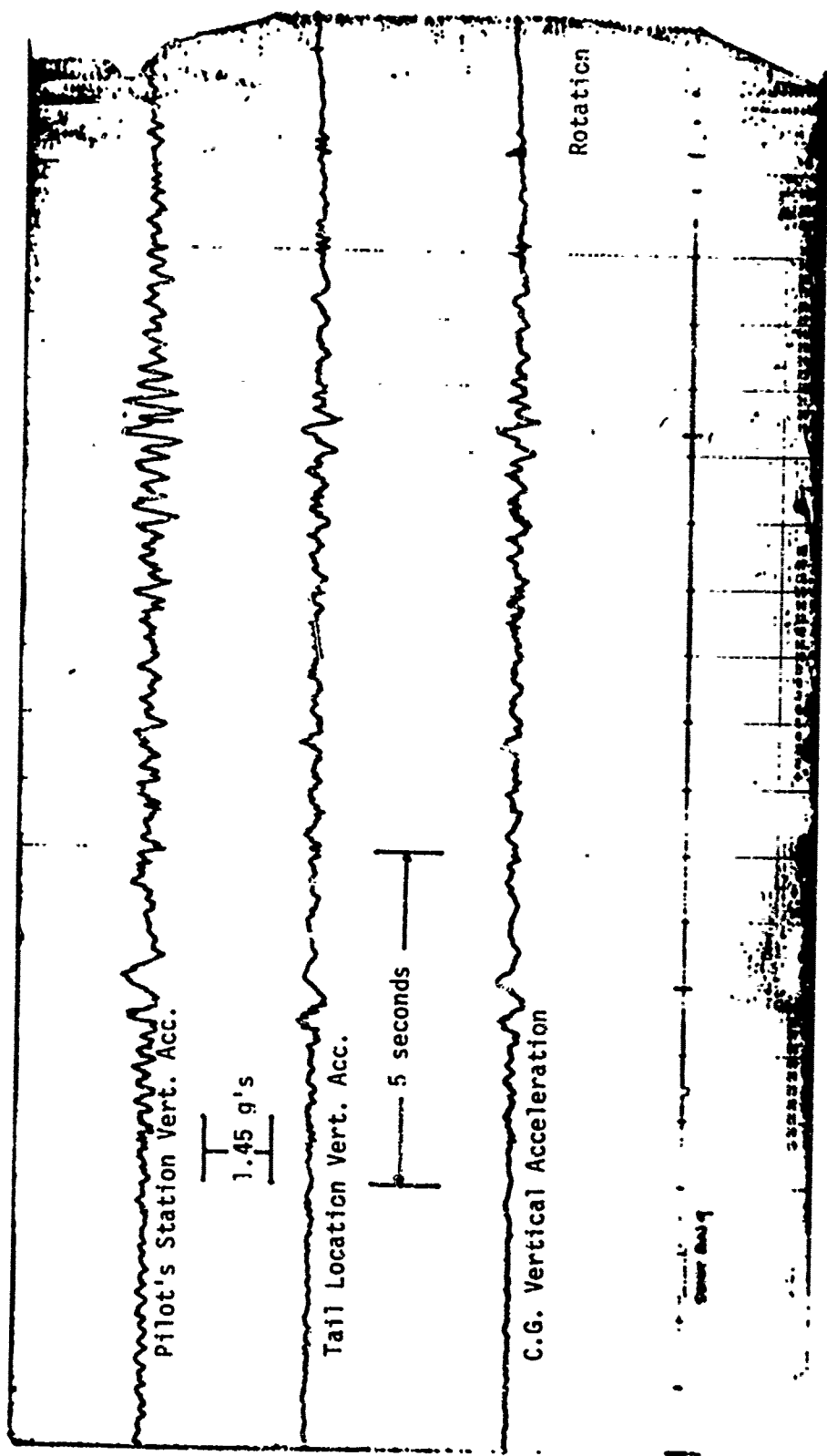


Figure 16. Measured Response of a Boeing 727-100 Takeoff at Washington National Airport Runway 36

TABLE 4  
COMPARISONS OF SIMULATED AND EXPERIMENTAL DATA

Experimental Time (sec)	P.S. Vertical Acceleration		C.G. Vertical Acceleration	
	Exp (g's)	Sim (g's)	Exp (g's)	Sim (g's)
8.0	0.9425	0.90	0.55	0.35
16.3	1.305	1.12	0.80	0.40
20.5		TAKEOF		

Note: All measurements are measured from peak to peak.

The remaining simulations made were with the inclusion of wing flexibility in the simulations. The purpose of including the wing flexibility was to see if there was a significant change in P.S. and C.G. vertical acceleration response when the wing was permitted to bend when acted on by a main landing gear strut force. These simulations were made on the C-9A only because this was the only aircraft for which wing flexibility data was available. Figure 17 shows the plotted results of C-9A with flexible wings traversing the 1-cos dip at a 45° angle. This figure can be compared to Figure 10 which is the same simulation without flexible wings. By superimposing the two plots it was determined after T=17 seconds, small changes in vertical acceleration were appearing in both the P.S. and C.G. responses. Generally the higher accelerations occurred on the C-9A simulation with flexible wings. Also there was a phase lag. By the end of the run the rigid wing model lagged the flexible wing model by approximately one half of a cycle. Figure 18 shows the plotted response of the C-9A with flexible wings during a takeoff simulation from Washington National Runway 36. Figure 14 shows the same simulation without flexible wings. Superposition of the two plots shows little change, if any, in the airplane's response.

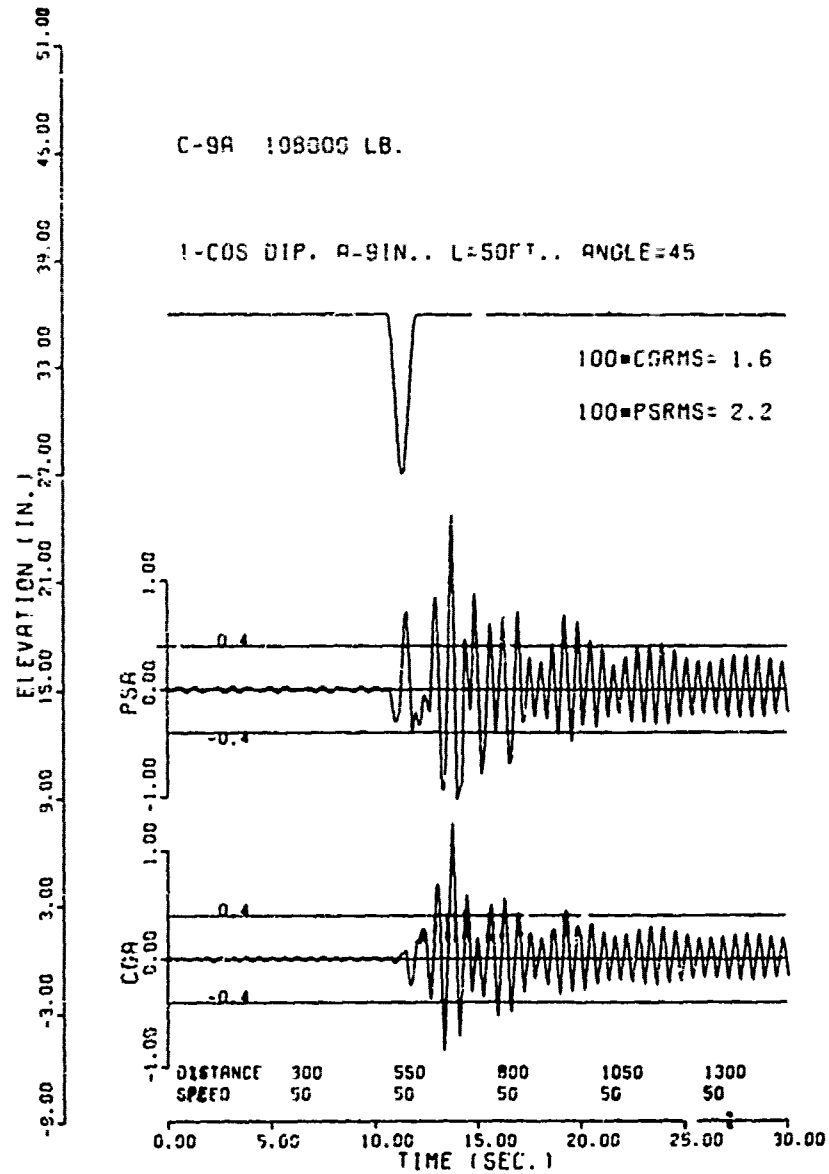


Figure 17. C-9A with Flexible Wings Taxiing over a (1-cos) dip at a 45° angle

AFFDL-TR-77-37

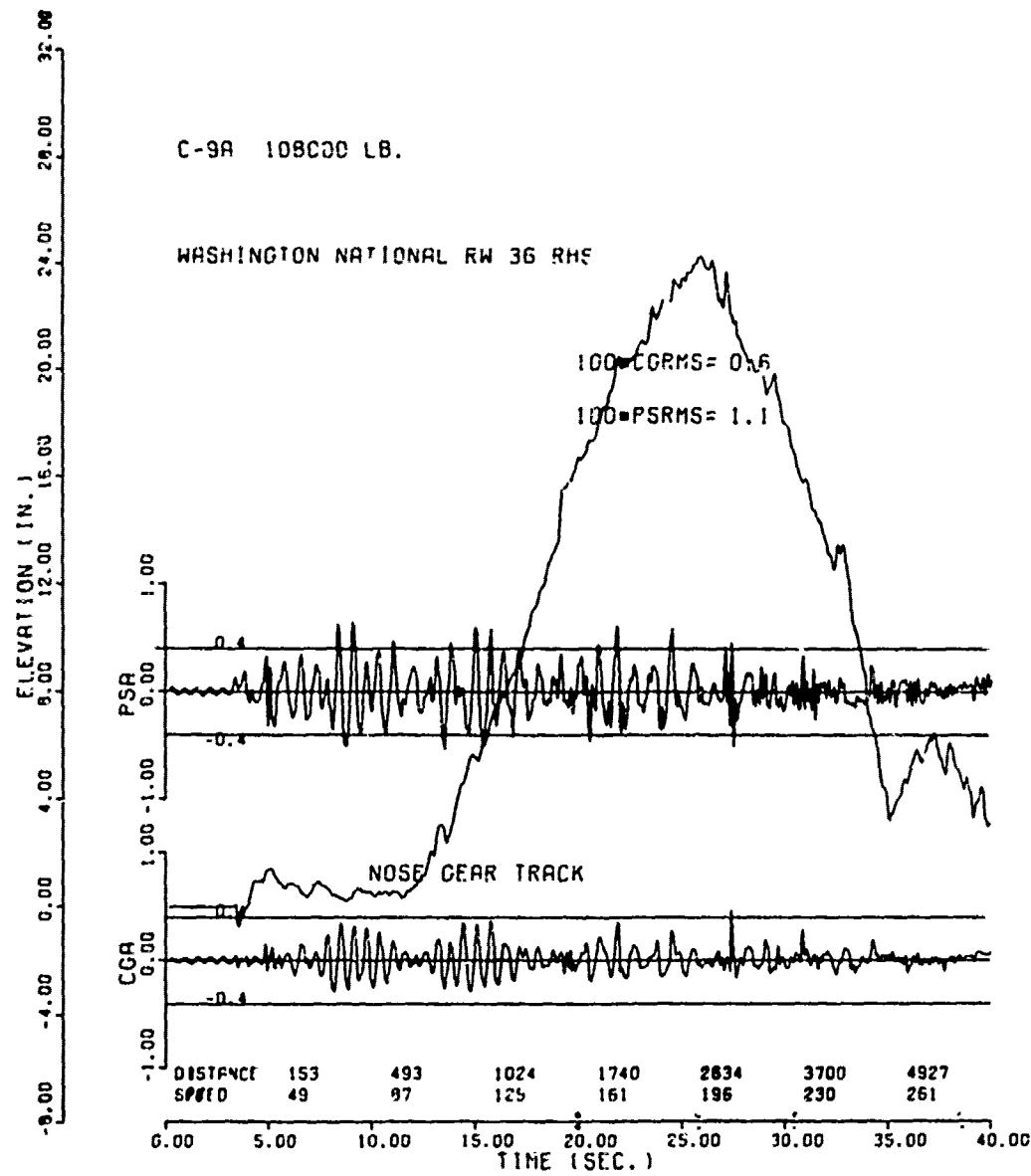


Figure 18. C-9A with Flexible Wings Taking Off from Washington National Runway 36

SECTION V  
SUMMARY AND CONCLUSIONS

In summary, a mathematical model has been formulated and programmed for a digital computer and is capable of simulating most flexible aircraft traversing an unsymmetric runway profile during constant speed taxi or takeoff. Three different aircraft have been simulated and comparisons have been made with experimental data.

Based on the 11 simulations made, the following conclusions were drawn:

1. The roll degree of freedom has a significant effect on the pilot's station and center of gravity vertical acceleration levels if the runway profile is asymmetric. The degree is dependent upon how asymmetric the profile is.
2. The effect of wing flexibility on F.S. and C.G. vertical acceleration response is small enough to be neglected, at least for the airplane simulated (C-9A). However, with the addition of flexible wings, it now becomes an easy matter to expand the computer program to obtain vertical accelerations (and consequently shears and moments) at vital wing stations such as the wing root and engine and stores pylons. This would be a natural extension of the study.
3. Comparison of the simulated aircraft response with the limited amount of available test data was satisfactory. The roughest parts of the runway were identified and, as in the test, pilot station acceleration levels exceeded the  $\pm 0.4g$  criterion. If exact strut and tire pressures, and inertia's were known for the test aircraft, the simulated C.G. response may have more closely matched the experimental data.

The simulated takeoff took an additional 5 seconds to reach rotation speed. It is assumed that the actual test aircraft weight was less than 120,000 pounds, because several runs were made without refueling the aircraft after each run. Therefore, some of the fuel had been burned off. The fact that the airplane was lighter than

that simulated would also contribute to the difference in C.G. response. Also, using a 15° flap setting changed the value of  $C_L$  and resulted in a shorter takeoff distance.

4. This computer program, "TAX2", appears to be a very efficient technique for locating the rough areas of an asymmetric runway. Using a CDC 6600 digital computer, a C-9A takeoff simulation required 70 seconds of central processor (CP) computer time, which is just 30 seconds over real time for this simulation. These numbers are typical for most simulations.

One of the advantages of a program of this type is that runway repairs can be simulated before the actual repair is made in order to determine the minimum amount of repair required. In addition, the effect of the proposed repair on other aircraft can be determined before the repair is made.

APPENDIX A  
DEVELOPMENT OF EQUATIONS OF MOTION

Development of equations of motion using Lagrange equations. All symbols refer to Figure A-1.

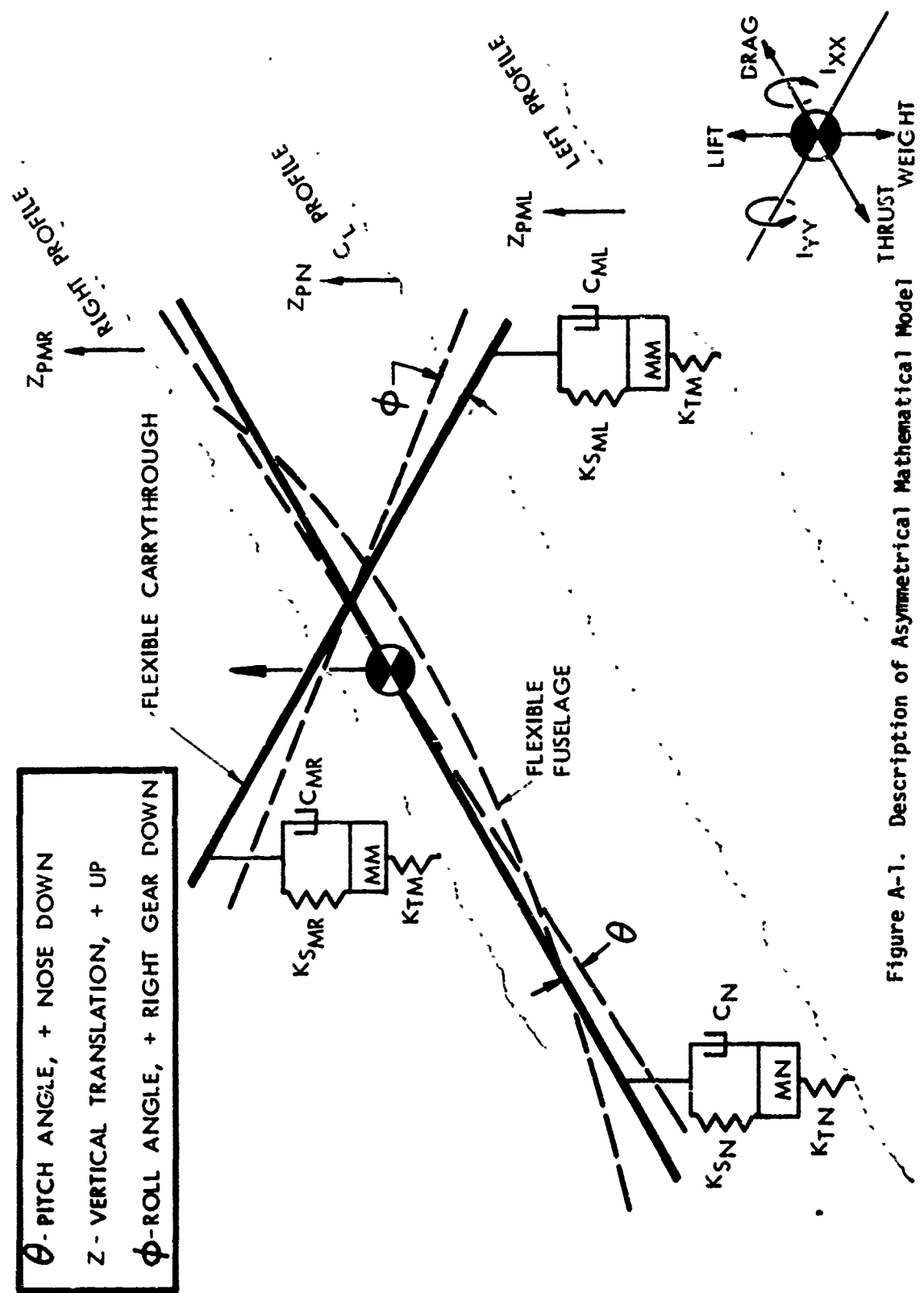


Figure A-1. Description of Asymmetrical Mathematical Model

Using Lagrange

$$\frac{d}{dt} \frac{\partial KE}{\partial \dot{q}_i} - \frac{\partial KE}{\partial q_i} + \frac{\partial PE}{\partial q_i} + \frac{\partial DE}{\partial \dot{q}_i} = 0$$

The Kinetic Energy is:

$$K.E. = \frac{1}{2} M_{cg} \dot{z}_{MR}^2 + \frac{1}{2} M_{ML} \dot{z}_{ML}^2 \\ + \frac{1}{2} M_N \dot{z}_N^2 + \frac{1}{2} I_{yy} \dot{\theta}^2 + \frac{1}{2} I_{xx} \dot{\phi}^2$$

The Potential Energy is:

$$P.E. = + W_M z_{MR} + W_M z_{ML} + W_N z_N + W_{cg} z_{cg} - L z_{cg} \\ + \frac{1}{2} K_{SML} (z_{cg} + A\theta - z_{ML} - C\phi)^2 + \frac{1}{2} K_{T1} (z_{ML} - z_{PMI})^2 \\ + \frac{1}{2} K_{SMR} (z_{cg} + A\theta - z_{MR} + C\phi)^2 + \frac{1}{2} K_{TM} (z_{MR} - z_{PMR})^2 \\ + \frac{1}{2} K_{SN} (z_{cg} - B\theta - z_N)^2 + \frac{1}{2} K_{TN} (z_N - z_{PN})^2$$

The Dissipative Energy is:

$$D.E. = + \frac{1}{2} C_{ML} (\dot{z}_{cg} + A\dot{\theta} - \dot{z}_{ML} - C\dot{\phi})^2 \\ + \frac{1}{2} C_{MR} (\dot{z}_{cg} + A\dot{\theta} - \dot{z}_{MR} + C\dot{\phi})^2 \\ + \frac{1}{2} C_N (\dot{z}_{cg} - B\dot{\theta} - \dot{z}_N)^2$$

Now Find  $\frac{d}{dt} \frac{\partial KE}{\partial \dot{q}_i}$ 

$$\frac{d}{dt} \frac{\partial KE}{\partial \dot{z}_{cg}} = M_{cg} \ddot{z}_{cg}; \quad \frac{d}{dt} \frac{\partial KE}{\partial \dot{z}_N} = M_N \ddot{z}_N$$

$$\frac{d}{dt} \frac{\partial KE}{\partial \dot{z}_{MR}} = M_{ML} \ddot{z}_{MR}; \quad \frac{d}{dt} \frac{\partial KE}{\partial \dot{\theta}} = I_{yy} \ddot{\theta}$$

$$\frac{d}{dt} \frac{\partial KE}{\partial \dot{z}_{ML}} = M_{ML} \ddot{z}_{ML}; \quad \frac{d}{dt} \frac{\partial KE}{\partial \dot{\phi}} = I_{xx} \ddot{\phi}$$

$$\frac{\partial KE}{\partial q_i} = 0$$

Now Find  $\frac{\partial(P.E)}{\partial q_i}$ 

$$\frac{\partial(P.E)}{\partial z_{cg}} = + K_{SML}(z_{cg} + A\theta - z_{ML} - C\phi)$$

$$+ K_{SMR}(z_{cg} + A\theta - z_{MR} + C\phi)$$

$$+ K_{SN}(z_{cg} - B\theta - z_N) + W - L$$

$$\frac{\partial(P.E)}{\partial z_{MR}} = + W_M - K_{SMR}(z_{cg} + A\theta - z_{MR} + C\phi)$$

$$+ K_{TM}(z_{MR} - z_{PMR})$$

$$\frac{\partial(P.E)}{\partial z_{ML}} = + W_M - K_{SML}(z_{cg} + A\theta - z_{ML} - C\phi)$$

$$+ K_{TM}(z_{ML} - z_{PML})$$

$$\frac{\partial(P.E)}{\partial z_N} = + W_N - K_{SN}(z_{cg} - B\theta - z_N) + K_{TN}(z_N - z_{PN})$$

$$\frac{\partial(P.E)}{\partial \dot{\theta}} = + K_{SML}A(z_{cg} + A\theta - z_{ML} - C\phi)$$

$$+ K_{SMR}A(z_{cg} + A\theta - z_{MR} + C\phi)$$

$$- K_{SN}B(z_{cg} - B\theta - z_N)$$

$$\frac{\partial(P.E)}{\partial \dot{\phi}} = - K_{SML}C(z_{cg} + A\theta - z_{ML} - C\phi)$$

$$+ K_{SMR}C(z_{cg} + A\theta - z_{MR} + C\phi)$$

Now Find  $\frac{\partial(D.E)}{\partial \dot{q}_i}$ 

$$\frac{\partial(D.E)}{\partial \dot{z}_{MR}} = - C_{MR}(\dot{z}_{cg} + A\dot{\theta} - \dot{z}_{MR} + C\dot{\phi})$$

$$\frac{\partial(D.E)}{\partial \dot{z}_{ML}} = - C_{ML} (\dot{z}_{cg} + A\dot{\theta} - \dot{z}_{ML} - C\dot{\phi})$$

$$\frac{\partial(D.E)}{\partial \dot{z}_N} = - C_N (\dot{z}_{cg} - B\dot{\theta} - \dot{z}_N)$$

$$\begin{aligned} \frac{\partial(D.E)}{\partial \dot{z}_{cg}} &= + C_{MR} (\dot{z}_{cg} + A\dot{\theta} - \dot{z}_{MR} + C\dot{\phi}) \\ &\quad + C_{ML} (\dot{z}_{cg} + A\dot{\theta} - \dot{z}_{ML} - C\dot{\phi}) \\ &\quad - C_N (\dot{z}_{cg} - B\dot{\theta} - \dot{z}_N) \end{aligned}$$

$$\begin{aligned} \frac{\partial(D.E)}{\partial \dot{\theta}} &= + C_{MR} A (\dot{z}_{cg} + A\dot{\theta} - \dot{z}_{MR} + C\dot{\phi}) \\ &\quad + C_{ML} A (\dot{z}_{cg} + A\dot{\theta} - \dot{z}_{ML} - C\dot{\phi}) \\ &\quad - C_N B (\dot{z}_{cg} - B\dot{\theta} - \dot{z}_N) \end{aligned}$$

$$\begin{aligned} \frac{\partial(D.E)}{\partial \dot{\phi}} &= + C_{MR} C (\dot{z}_{cg} + A\dot{\theta} - \dot{z}_{MR} + C\dot{\phi}) \\ &\quad - C_{ML} C (\dot{z}_{cg} + A\dot{\theta} - \dot{z}_{MR} - C\dot{\phi}) \end{aligned}$$

Combine Terms

$$\begin{aligned} \ddot{M}\dot{z}_{cg} &= - K_{SML} [z_{cg} + A\dot{\theta} - z_{ML} - C\dot{\phi}] \\ &\quad - K_{SMR} [z_{cg} + A\dot{\theta} - z_{MR} + C\dot{\phi}] \\ &\quad - K_{SN} [z_{cg} - B\dot{\theta} - z_N] - W + L \\ &\quad - C_{MR} [\dot{z}_{cg} + A\dot{\theta} - \dot{z}_{MR} + C\dot{\phi}] \\ &\quad - C_{ML} [\dot{z}_{cg} + A\dot{\theta} - \dot{z}_{ML} - C\dot{\phi}] \\ &\quad - C_N [\dot{z}_{cg} - B\dot{\theta} - \dot{z}_N] \end{aligned}$$

Rewriting we have

$$\ddot{M}\dot{z}_{cg} = [-K_{SML}(x_{ML}) - C_{ML}(x_{ML})] + \quad (1)$$

$$[-K_{SMR}(x_{MR}) - C_{MR}(\dot{x}_{MR})] + \\ [-K_{SN}(x_N) - C_N(\dot{x}_N)] = W + L$$

where the terms in the brackets are the left, right, and nose landing gear strut forces respectively.

Similarly

$$\ddot{M_z}_{ML} = K_{SML}(x_{ML}) + C_{ML}(\dot{x}_{ML}) \\ - K_{TM}(z_{ML} - z_{PML}) - W_M \quad (2)$$

$$\ddot{M_z}_{MR} = K_{SMR}(x_{MR}) + C_{MR}(\dot{x}_{MR}) \\ - K_{TM}(z_{MR} - z_{PMR}) - W_M \quad (3)$$

$$\ddot{M_z}_N = K_{SN}(x_N) + C_N(\dot{x}_N) - K_{TN}(z_N - z_{PN}) \quad (4)$$

$$\ddot{I_{yy}\theta} = -K_{SML}A(x_{ML}) + C_{ML}A(\dot{x}_{ML}) \\ + K_{SMR}A(x_{MR}) + C_{MR}A(\dot{x}_{MR}) \\ - K_NB(x_N) + C_NB(\dot{x}_N) \quad (5)$$

$$\ddot{I_{xy}\phi} = K_{SML}C(x_{ML}) + C_{ML}C(\dot{x}_{ML}) \\ - K_{SMR}C(x_{MR}) - C_{MR}C(\dot{x}_{MR}) \quad (6)$$

The Forward Translation Equation of Motion is uncoupled and expressed as follows:

$$\ddot{MX} = T - D_a - D_t$$

where:

T = Thrust

$D_a$  = Aerodynamic Drag

$D_t$  = Tire Drag (Total)

The modal method will be used to express the aircraft's flexibility as follows:

$$\ddot{M_i q_i} = \xi_{ij} F_j - 2\zeta\omega_i \dot{M_i q_i} - \omega_i^2 M_i q_i$$

where  $i$  = the  $i$ th mode

$F_j$  = the  $j$ th force input into the system (such as strut force)

$M_i$  = the  $i$ th generalized mass

$q_i$  = the generalized coordinate

$\xi_{ij}$  = the modal deflection of the  $i$ th mode at fuselage station  $j$  for symmetric modes or wing station  $j$  for asymmetric modes.

$\omega_i$  = the  $i$ th mode natural frequency

$\zeta$  = Structural damping factor

By using this technique the displacements  $X'_{MR}$ ,  $X'_{ML}$ ,  $X'_{N}$  and their time derivatives reflect the motion of the bending fuselage and wings by adding the  $\sum_{i=1}^N q_i \xi_{ij}$  (modal displacements) at the  $j$ th (required location).

For example;

$$\text{Total Displacement } X'_{MR} = X_{MR} + \sum_{i=1}^N q_i \xi_{iR} + \sum_{k=1}^P q_k \xi_{kR}$$

$$\text{Total Velocity } \dot{X}'_{MR} = \dot{X}_{MR} + \sum_{i=1}^N \dot{q}_i \xi_{iR} + \sum_{k=1}^P \dot{q}_k \xi_{kR}$$

where:

Term 1 = Displacements of the rigid body

Term 2 = Displacements due to the symmetric modes

Term 3 = Displacements due to the asymmetric modes

AFFDL-TR-77-37

APPENDIX B  
LISTING OF COMPUTER PROGRAM TAX2

**BEST AVAILABLE COPY**

**BEST AVAILABLE COPY**

	RTN 4.7-3496	RTN 4.7-22-24	PAGE
42	C DISTANCE MAIN GEAR TO CG (INCHES) C DISTANCE MODE GEAR TO CG (INCHES)	TAX2040 TAX2050	2
43	C WING STATION IN (INCHES) C WING WING MOMENT OF INERTIA IN OULDS IN SFC - SOI	TAX2050 TAX2050	
44	C PLANE, AIRPLANE BEING STUDIED AND MASS DRAFT	TAX2050	
45	C PILOT - DISTANCE OF PILOT STATION TO CG	TAX2050	
46	C TAIL - DISTANCE OF TAIL STATION TO CG	TAX2050	
47	C TOWER TAKE-OFF SPEED (FEET/SEC)	TAX2050	
48	C SPEED INITIAL (FT. OF FREIGHT)	TAX2050	
49	C THRUST TOTAL AIRPLANE (NEWTONS)	TAX2050	
50	C CLUTCH COUPLE	TAX2050	
51	C BREAKING AREA	TAX2050	
52	C CRASHING COUPLE	TAX2050	
53	C WEIGHT OF MAIN GEAR (POUNDS)	TAX2050	
54	C WEIGHT OF TAIL GEAR (POUNDS)	TAX2050	
55	C SAME NUMBER OF MAIN GEAR STRUTS	TAX2050	
56	C SAME NUMBER OF TAIL GEAR STRUTS	TAX2050	
57	C HOUSING HYDRAULIC PISTON AREA (INCHES <sup>2</sup> )	TAX2050	
58	C HOUSING PNEUMATIC PISTON AREA (INCHES <sup>2</sup> )	TAX2050	
59	C HOUSING PNEUMATIC PISTON AREA (INCHES <sup>2</sup> )	TAX2050	
60	C HOUSING PNEUMATIC PISTON AREA (INCHES <sup>2</sup> )	TAX2050	
61	C HOSE HOSE STRUT LOAD PRESSURE (PSI)	TAX2050	
62	C EACH MAIN STRUT LOAD PRESSURE (PSI)	TAX2050	
63	C VON HOSE STRUT INITIAL VOLUME (CU. IN.)	TAX2050	
64	C HOSE STRUT INITIAL VOLUME (CU. IN.)	TAX2050	
65	C SURFACE AREA MAIN	TAX2050	
66	C SURFACE AREA NOSE	TAX2050	
67	C SURFACE AREA TAIL	TAX2050	
68	C SURFACE AREA CRASH LEGACY UNLOADING LENGTH'S	TAX2050	
69	C DISTANCE FROM CL OF AXLE TO CL LINE	TAX2050	
70	C SURFACE GEAR STRUT LENGTH UNLOADING LENGTH'S	TAX2050	
71	C DISTANCE FROM CL OF AXLE TO CL LINE	TAX2050	
72	C TAN TIRE SPRING CONSTANT PER STRUT	TAX2050	
73	C TSM HOSE TIRE SPRINGS CONSTANT PER STRUT	TAX2050	
74	C BRAKE STEER SITE	TAX2050	
75	C BRAKE ACTUATOR PIN DESCRIPTION STARTING AT 220° STROKE	TAX2050	
76	C NUMBER OF METALING PIN CHAMPS NOSE GEAR	TAX2050	
77	C NUMBER OF METALING PIN CHAMPS MAIN GEAR	TAX2050	
78	C NUMBER OF FLEXIBLE MODES	TAX2050	
79	C NUMBER OF ASYMETRIC MODES	TAX2050	
80	C SURFACE (A) = MODE SHAPE DEFLECTION (RAD/SEC)	TAX2050	
81	C SURFACE (B) = MODAL FREQUENCIES (RAD/SEC)	TAX2050	
82	C SURFACE (C) = MODE SHAPE DEFLECTION	TAX2050	
83	C STRAIGHT - LEFT GEAR MODE SHAPE DEFLECTION	TAX2050	
84	C STRAIGHT - RIGHT GEAR MODE SHAPE DEFLECTION	TAX2050	
85	C CRASH - 45°, MODE REV. MASS	TAX2050	
86	C ONE-GEAR-UP ASYN. MODE FREQ.	TAX2050	
87	C READ (5,11) PLACE	TAX2050	
88	C FORWARD: 31, 41, 51, 61, 71, 81, 91, 101, 111, 121, 131, 141, 151, 161, 171, 181, 191, 201, 211, 221, 231, 241, 251, 261, 271, 281, 291, 301, 311, 321, 331, 341, 351, 361, 371, 381, 391, 401, 411, 421, 431, 441, 451, 461, 471, 481, 491, 501, 511, 521, 531, 541, 551, 561, 571, 581, 591, 601, 611, 621, 631, 641, 651, 661, 671, 681, 691, 701, 711, 721, 731, 741, 751, 761, 771, 781, 791, 801, 811, 821, 831, 841, 851, 861, 871, 881, 891, 901, 911, 921, 931, 941, 951, 961, 971, 981, 991, 1011, 1021, 1031, 1041, 1051, 1061, 1071, 1081, 1091, 1101, 1111, 1121, 1131, 1141, 1151, 1161, 1171, 1181, 1191, 1201, 1211, 1221, 1231, 1241, 1251, 1261, 1271, 1281, 1291, 1301, 1311, 1321, 1331, 1341, 1351, 1361, 1371, 1381, 1391, 1401, 1411, 1421, 1431, 1441, 1451, 1461, 1471, 1481, 1491, 1501, 1511, 1521, 1531, 1541, 1551, 1561, 1571, 1581, 1591, 1601, 1611, 1621, 1631, 1641, 1651, 1661, 1671, 1681, 1691, 1701, 1711, 1721, 1731, 1741, 1751, 1761, 1771, 1781, 1791, 1801, 1811, 1821, 1831, 1841, 1851, 1861, 1871, 1881, 1891, 1901, 1911, 1921, 1931, 1941, 1951, 1961, 1971, 1981, 1991, 2001, 2011, 2021, 2031, 2041, 2051, 2061, 2071, 2081, 2091, 2101, 2111, 2121, 2131, 2141, 2151, 2161, 2171, 2181, 2191, 2201, 2211, 2221, 2231, 2241, 2251, 2261, 2271, 2281, 2291, 2301, 2311, 2321, 2331, 2341, 2351, 2361, 2371, 2381, 2391, 2401, 2411, 2421, 2431, 2441, 2451, 2461, 2471, 2481, 2491, 2501, 2511, 2521, 2531, 2541, 2551, 2561, 2571, 2581, 2591, 2601, 2611, 2621, 2631, 2641, 2651, 2661, 2671, 2681, 2691, 2701, 2711, 2721, 2731, 2741, 2751, 2761, 2771, 2781, 2791, 2801, 2811, 2821, 2831, 2841, 2851, 2861, 2871, 2881, 2891, 2901, 2911, 2921, 2931, 2941, 2951, 2961, 2971, 2981, 2991, 3001, 3011, 3021, 3031, 3041, 3051, 3061, 3071, 3081, 3091, 3101, 3111, 3121, 3131, 3141, 3151, 3161, 3171, 3181, 3191, 3201, 3211, 3221, 3231, 3241, 3251, 3261, 3271, 3281, 3291, 3301, 3311, 3321, 3331, 3341, 3351, 3361, 3371, 3381, 3391, 3401, 3411, 3421, 3431, 3441, 3451, 3461, 3471, 3481, 3491, 3501, 3511, 3521, 3531, 3541, 3551, 3561, 3571, 3581, 3591, 3601, 3611, 3621, 3631, 3641, 3651, 3661, 3671, 3681, 3691, 3701, 3711, 3721, 3731, 3741, 3751, 3761, 3771, 3781, 3791, 3801, 3811, 3821, 3831, 3841, 3851, 3861, 3871, 3881, 3891, 3901, 3911, 3921, 3931, 3941, 3951, 3961, 3971, 3981, 3991, 4001, 4011, 4021, 4031, 4041, 4051, 4061, 4071, 4081, 4091, 4101, 4111, 4121, 4131, 4141, 4151, 4161, 4171, 4181, 4191, 4201, 4211, 4221, 4231, 4241, 4251, 4261, 4271, 4281, 4291, 4301, 4311, 4321, 4331, 4341, 4351, 4361, 4371, 4381, 4391, 4401, 4411, 4421, 4431, 4441, 4451, 4461, 4471, 4481, 4491, 4501, 4511, 4521, 4531, 4541, 4551, 4561, 4571, 4581, 4591, 4601, 4611, 4621, 4631, 4641, 4651, 4661, 4671, 4681, 4691, 4701, 4711, 4721, 4731, 4741, 4751, 4761, 4771, 4781, 4791, 4801, 4811, 4821, 4831, 4841, 4851, 4861, 4871, 4881, 4891, 4901, 4911, 4921, 4931, 4941, 4951, 4961, 4971, 4981, 4991, 5001, 5011, 5021, 5031, 5041, 5051, 5061, 5071, 5081, 5091, 5101, 5111, 5121, 5131, 5141, 5151, 5161, 5171, 5181, 5191, 5201, 5211, 5221, 5231, 5241, 5251, 5261, 5271, 5281, 5291, 5301, 5311, 5321, 5331, 5341, 5351, 5361, 5371, 5381, 5391, 5401, 5411, 5421, 5431, 5441, 5451, 5461, 5471, 5481, 5491, 5501, 5511, 5521, 5531, 5541, 5551, 5561, 5571, 5581, 5591, 5501, 5511, 5521, 5531, 5541, 5551, 5561, 5571, 5581, 5591, 5601, 5611, 5621, 5631, 5641, 5651, 5661, 5671, 5681, 5691, 5601, 5611, 5621, 5631, 5641, 5651, 5661, 5671, 5681, 5691, 5701, 5711, 5721, 5731, 5741, 5751, 5761, 5771, 5781, 5791, 5701, 5711, 5721, 5731, 5741, 5751, 5761, 5771, 5781, 5791, 5801, 5811, 5821, 5831, 5841, 5851, 5861, 5871, 5881, 5891, 5801, 5811, 5821, 5831, 5841, 5851, 5861, 5871, 5881, 5891, 5901, 5911, 5921, 5931, 5941, 5951, 5961, 5971, 5981, 5991, 5901, 5911, 5921, 5931, 5941, 5951, 5961, 5971, 5981, 5991, 6001, 6011, 6021, 6031, 6041, 6051, 6061, 6071, 6081, 6091, 6001, 6011, 6021, 6031, 6041, 6051, 6061, 6071, 6081, 6091, 6101, 6111, 6121, 6131, 6141, 6151, 6161, 6171, 6181, 6191, 6101, 6111, 6121, 6131, 6141, 6151, 6161, 6171, 6181, 6191, 6201, 6211, 6221, 6231, 6241, 6251, 6261, 6271, 6281, 6291, 6201, 6211, 6221, 6231, 6241, 6251, 6261, 6271, 6281, 6291, 6301, 6311, 6321, 6331, 6341, 6351, 6361, 6371, 6381, 6391, 6301, 6311, 6321, 6331, 6341, 6351, 6361, 6371, 6381, 6391, 6401, 6411, 6421, 6431, 6441, 6451, 6461, 6471, 6481, 6491, 6401, 6411, 6421, 6431, 6441, 6451, 6461, 6471, 6481, 6491, 6501, 6511, 6521, 6531, 6541, 6551, 6561, 6571, 6581, 6591, 6501, 6511, 6521, 6531, 6541, 6551, 6561, 6571, 6581, 6591, 6601, 6611, 6621, 6631, 6641, 6651, 6661, 6671, 6681, 6691, 6601, 6611, 6621, 6631, 6641, 6651, 6661, 6671, 6681, 6691, 6701, 6711, 6721, 6731, 6741, 6751, 6761, 6771, 6781, 6791, 6701, 6711, 6721, 6731, 6741, 6751, 6761, 6771, 6781, 6791, 6801, 6811, 6821, 6831, 6841, 6851, 6861, 6871, 6881, 6891, 6801, 6811, 6821, 6831, 6841, 6851, 6861, 6871, 6881, 6891, 6901, 6911, 6921, 6931, 6941, 6951, 6961, 6971, 6981, 6991, 6901, 6911, 6921, 6931, 6941, 6951, 6961, 6971, 6981, 6991, 7001, 7011, 7021, 7031, 7041, 7051, 7061, 7071, 7081, 7091, 7001, 7011, 7021, 7031, 7041, 7051, 7061, 7071, 7081, 7091, 7101, 7111, 7121, 7131, 7141, 7151, 7161, 7171, 7181, 7191, 7101, 7111, 7121, 7131, 7141, 7151, 7161, 7171, 7181, 7191, 7201, 7211, 7221, 7231, 7241, 7251, 7261, 7271, 7281, 7291, 7201, 7211, 7221, 7231, 7241, 7251, 7261, 7271, 7281, 7291, 7301, 7311, 7321, 7331, 7341, 7351, 7361, 7371, 7381, 7391, 7301, 7311, 7321, 7331, 7341, 7351, 7361, 7371, 7381, 7391, 7401, 7411, 7421, 7431, 7441, 7451, 7461, 7471, 7481, 7491, 7401, 7411, 7421, 7431, 7441, 7451, 7461, 7471, 7481, 7491, 7501, 7511, 7521, 7531, 7541, 7551, 7561, 7571, 7581, 7591, 7501, 7511, 7521, 7531, 7541, 7551, 7561, 7571, 7581, 7591, 7601, 7611, 7621, 7631, 7641, 7651, 7661, 7671, 7681, 7691, 7601, 7611, 7621, 7631, 7641, 7651, 7661, 7671, 7681, 7691, 7701, 7711, 7721, 7731, 7741, 7751, 7761, 7771, 7781, 7791, 7701, 7711, 7721, 7731, 7741, 7751, 7761, 7771, 7781, 7791, 7801, 7811, 7821, 7831, 7841, 7851, 7861, 7871, 7881, 7891, 7801, 7811, 7821, 7831, 7841, 7851, 7861, 7871, 7881, 7891, 7901, 7911, 7921, 7931, 7941, 7951, 7961, 7971, 7981, 7991, 7901, 7911, 7921, 7931, 7941, 7951, 7961, 7971, 7981, 7991, 8001, 8011, 8021, 8031, 8041, 8051, 8061, 8071, 8081, 8091, 8001, 8011, 8021, 8031, 8041, 8051, 8061, 8071, 8081, 8091, 8101, 8111, 8121, 8131, 8141, 8151, 8161, 8171, 8181, 8191, 8101, 8111, 8121, 8131, 8141, 8151, 8161, 8171, 8181, 8191, 8201, 8211, 8221, 8231, 8241, 8251, 8261, 8271, 8281, 8291, 8201, 8211, 8221, 8231, 8241, 8251, 8261, 8271, 8281, 8291, 8301, 8311, 8321, 8331, 8341, 8351, 8361, 8371, 8381, 8391, 8301, 8311, 8321, 8331, 8341, 8351, 8361, 8371, 8381, 8391, 8401, 8411, 8421, 8431, 8441, 8451, 8461, 8471, 8481, 8491, 8401, 8411, 8421, 8431, 8441, 8451, 8461, 8471, 8481, 8491, 8501, 8511, 8521, 8531, 8541, 8551, 8561, 8571, 8581, 8591, 8501, 8511, 8521, 8531, 8541, 8551, 8561, 8571, 8581, 8591, 8601, 8611, 8621, 8631, 8641, 8651, 8661, 8671, 8681, 8691, 8601, 8611, 8621, 8631, 8641, 8651, 8661, 8671, 8681, 8691, 8701, 8711, 8721, 8731, 8741, 8751, 8761, 8771, 8781, 8791, 8701, 8711, 8721, 8731, 8741, 8751, 8761, 8771, 8781, 8791, 8801, 8811, 8821, 8831, 8841, 8851, 8861, 8871, 8881, 8891, 8801, 8811, 8821, 8831, 8841, 8851, 8861, 8871, 8881, 8891, 8901, 8911, 8921, 8931, 8941, 8951, 8961, 8971, 8981, 8991, 8901, 8911, 8921, 8931, 8941, 8951, 8961, 8971, 8981, 8991, 9001, 9011, 9021, 9031, 9041, 9051, 9061, 9071, 9081, 9091, 9001, 9011, 9021, 9031, 9041, 9051, 9061, 9071, 9081, 9091, 9101, 9111, 9121, 9131, 9141, 9151, 9161, 9171, 9181, 9191, 9101, 9111, 9121, 9131, 9141, 9151, 9161, 9171, 9181, 9191, 9201, 9211, 9221, 9231, 9241, 9251, 9261, 9271, 9281, 9291, 9201, 9211, 9221, 9231, 9241, 9251, 9261, 9271, 9281, 9291, 9301, 9311, 9321, 9331, 9341, 9351, 9361, 9371, 9381, 9391, 9301, 9311, 9321, 9331, 9341, 9351, 9361, 9371, 9381, 9391, 9401, 9411, 9421, 9431, 9441, 9451, 9461, 9471, 9481, 9491, 9401, 9411, 9421, 9431, 9441, 9451, 9461, 9471, 9481, 9491, 9501, 9511, 9521, 9531, 9541, 9551, 9561, 9571, 9581, 9591, 9501, 9511, 9521, 9531, 9541, 9551, 9561, 9571, 9581, 9591, 9601, 9611, 9621, 9631, 9641, 9651, 9661, 9671, 9681, 9691, 9601, 9611, 9621, 9631, 9641, 9651, 9661, 9671, 9681, 9691, 9701, 9711, 9721, 9731, 9741, 9751, 9761, 9771, 9781, 9791, 9701, 9711, 9721, 9731, 9741, 9751, 9761, 9771, 9781, 9791, 9801, 9811, 9821, 9831, 9841, 9851, 9861, 9871, 9881, 9891, 9801, 9811, 9821, 9831, 9841, 9851, 9861, 9871, 9881, 9891, 9901, 9911, 9921, 9931, 9941, 9951, 9961, 9971, 9981, 9991, 9901, 9911, 9921, 9931, 9941, 9951, 9961, 9971, 9981, 9991, 10001, 10011, 10021, 10031, 10041, 10051, 10061, 10071, 10081, 10091, 10001, 10011, 10021, 10031, 10041, 10051, 10061, 10071, 10081, 10091, 10101, 10111, 10121, 10131, 10141, 10151, 10161, 10171, 10181, 10191, 1		

**BEST AVAILABLE COPY**

PROCNAME		TIME		PAGE	
		MM/DD/YY	HH:MM:SS	MM/DD/YY	HH:MM:SS
115		READ(5,25)	W4, W4, S4H5X4	TAU2159	
	FORMAT(5,2)			TAU2159	
116	READ(5,30)	A4H4A4H4AH, A4H		TAU2159	
	FORMAT(5,5)			TAU2159	
117	READ(5,35)	A4H, P4H, V4H, V4H, C4H, U		TAU2159	
	FORMAT(5,5)			TAU2159	
118	READ(5,30)	S4H5X4		TAU2200	
	FORMAT(5,3)			TAU2200	
119	READ(5,35)	T3H + T5H		TAU2200	
	FORMAT(5,3)			TAU2200	
120	READ(5,30)	C4H, S4H2		TAU2200	
	FORMAT(5,3)			TAU2200	
121	READ(5,32)	I3H4C4H2, P4H4W4H, I, I, I, R24H		TAU2209	
	FORMAT(5,3)			TAU2209	
122	READ(5,25)	B4, S4H		TAU2209	
	FORMAT(5,3)			TAU2209	
123	READ(5,32)	I3H4C4H2, P4H4W4H, I, I, I, R24H		TAU2209	
	FORMAT(5,3)			TAU2209	
124	READ(5,30)	W4H, S4H		TAU2209	
	FORMAT(5,3)			TAU2209	
125	READ(5,30)	W5CH		TAU2209	
	FORMAT(5,3)			TAU2209	
126	READ(5,32)	I3H4C4H2, P4H4W4H, I, I, I, R24H		TAU2209	
	FORMAT(5,3)			TAU2209	
127	READ(5,30)	W4H, S4H		TAU2209	
	FORMAT(5,3)			TAU2209	
128	READ(5,30)	W4H, S4H		TAU2209	
	FORMAT(5,3)			TAU2209	
129	READ(5,30)	W4H, S4H		TAU2209	
	FORMAT(5,3)			TAU2209	
130	READ(5,30)	W4H, S4H		TAU2209	
	FORMAT(5,3)			TAU2209	
131	READ(5,30)	W4H, S4H		TAU2209	
	FORMAT(5,3)			TAU2209	
132	READ(5,30)	W4H, S4H		TAU2209	
	FORMAT(5,3)			TAU2209	
133	READ(5,30)	W4H, S4H		TAU2209	
	FORMAT(5,3)			TAU2209	
134	READ(5,30)	W4H, S4H		TAU2209	
	FORMAT(5,3)			TAU2209	
135	READ(5,30)	W4H, S4H		TAU2209	
	FORMAT(5,3)			TAU2209	
136	READ(5,30)	W4H, S4H		TAU2209	
	FORMAT(5,3)			TAU2209	
137	READ(5,30)	W4H, S4H		TAU2209	
	FORMAT(5,3)			TAU2209	
138	READ(5,30)	W4H, S4H		TAU2209	
	FORMAT(5,3)			TAU2209	
139	READ(5,30)	W4H, S4H		TAU2209	
	FORMAT(5,3)			TAU2209	
140	READ(5,30)	W4H, S4H		TAU2209	
	FORMAT(5,3)			TAU2209	
141	READ(5,30)	W4H, S4H		TAU2209	
	FORMAT(5,3)			TAU2209	
142	READ(5,30)	W4H, S4H		TAU2209	
	FORMAT(5,3)			TAU2209	
143	READ(5,30)	W4H, S4H		TAU2209	
	FORMAT(5,3)			TAU2209	
144	READ(5,30)	W4H, S4H		TAU2209	
	FORMAT(5,3)			TAU2209	
145	READ(5,30)	W4H, S4H		TAU2209	
	FORMAT(5,3)			TAU2209	
146	READ(5,30)	W4H, S4H		TAU2209	
	FORMAT(5,3)			TAU2209	
147	READ(5,30)	W4H, S4H		TAU2209	
	FORMAT(5,3)			TAU2209	
148	READ(5,30)	W4H, S4H		TAU2209	
	FORMAT(5,3)			TAU2209	
149	READ(5,30)	W4H, S4H		TAU2209	
	FORMAT(5,3)			TAU2209	
150	READ(5,30)	W4H, S4H		TAU2209	
	FORMAT(5,3)			TAU2209	
151	READ(5,30)	W4H, S4H		TAU2209	
	FORMAT(5,3)			TAU2209	
152	READ(5,30)	W4H, S4H		TAU2209	
	FORMAT(5,3)			TAU2209	
153	READ(5,30)	W4H, S4H		TAU2209	
	FORMAT(5,3)			TAU2209	
154	READ(5,30)	W4H, S4H		TAU2209	
	FORMAT(5,3)			TAU2209	
155	READ(5,30)	W4H, S4H		TAU2209	
	FORMAT(5,3)			TAU2209	
156	READ(5,30)	W4H, S4H		TAU2209	
	FORMAT(5,3)			TAU2209	
157	READ(5,30)	W4H, S4H		TAU2209	
	FORMAT(5,3)			TAU2209	
158	READ(5,30)	W4H, S4H		TAU2209	
	FORMAT(5,3)			TAU2209	
159	READ(5,30)	W4H, S4H		TAU2209	
	FORMAT(5,3)			TAU2209	
160	READ(5,30)	W4H, S4H		TAU2209	
	FORMAT(5,3)			TAU2209	
161	READ(5,30)	W4H, S4H		TAU2209	
	FORMAT(5,3)			TAU2209	
162	READ(5,30)	W4H, S4H		TAU2209	
	FORMAT(5,3)			TAU2209	
163	READ(5,30)	W4H, S4H		TAU2209	
	FORMAT(5,3)			TAU2209	
164	READ(5,30)	W4H, S4H		TAU2209	
	FORMAT(5,3)			TAU2209	
165	READ(5,30)	W4H, S4H		TAU2209	
	FORMAT(5,3)			TAU2209	
166	READ(5,30)	W4H, S4H		TAU2209	
	FORMAT(5,3)			TAU2209	
167	READ(5,30)	W4H, S4H		TAU2209	
	FORMAT(5,3)			TAU2209	
168	READ(5,30)	W4H, S4H		TAU2209	
	FORMAT(5,3)			TAU2209	
169	READ(5,30)	W4H, S4H		TAU2209	
	FORMAT(5,3)			TAU2209	
170	READ(5,30)	W4H, S4H		TAU2209	
	FORMAT(5,3)			TAU2209	
171	READ(5,30)	W4H, S4H		TAU2209	
	FORMAT(5,3)			TAU2209	
172	READ(5,30)	W4H, S4H		TAU2209	
	FORMAT(5,3)			TAU2209	
173	READ(5,30)	W4H, S4H		TAU2209	
	FORMAT(5,3)			TAU2209	
174	READ(5,30)	W4H, S4H		TAU2209	
	FORMAT(5,3)			TAU2209	
175	READ(5,30)	W4H, S4H		TAU2209	
	FORMAT(5,3)			TAU2209	
176	READ(5,30)	W4H, S4H		TAU2209	
	FORMAT(5,3)			TAU2209	
177	READ(5,30)	W4H, S4H		TAU2209	
	FORMAT(5,3)			TAU2209	
178	READ(5,30)	W4H, S4H		TAU2209	
	FORMAT(5,3)			TAU2209	
179	READ(5,30)	W4H, S4H		TAU2209	
	FORMAT(5,3)			TAU2209	

BEST AVAILABLE COPY

**BEST AVAILABLE COPY**

**BEST AVAILABLE COPY**

**BEST AVAILABLE COPY**

# BEST AVAILABLE COPY

BEST AVAILABLE COPY

# BEST AVAILABLE COPY

**BEST AVAILABLE COPY**

**BEST AVAILABLE COPY**

BEST AVAILABLE COPY

SUBROUTINE CN	76774	09721	FTN 4.5+2406	05/25/775	17.22.26	PAGE
1	LOUTINE C2FFF (Y, 1,9,0,0)			C0FF010	CNEF020	
	IFN700 V(6)			CNEF030	C0FF040	
	ASY(2)			C0FF050	CNEF060	
	NY(1)			C0FF070	CNEF080	
5	C(-96.+V(1)+48.+V(2)-61.+V(3)+61.+V(4))/(-128.)			C0FF090		
	N(-L.+V(1)-12.+V(2)+15.+V(3)-4.+V(4))/(-128.)					
	REFURN					
	F40					

SUBROUTINE FLICK	76774	09721	FTN 4.5+2406	05/25/776	10.22.26	PAGE
1	SUBROUTINE FLICK (X, SLOPE, Y2201, Z2201)			TL 0010		
	DIMENSION S(10),P(10)			TL 0020		
5	C THIS IS A 2 DIMENSIONAL TABLE LOOK UP ROUTINE			TL 0030		
	WITH LINEAR INTERPOLATION			TL 0040		
	C X IS THE CURRENT VALUE OF STROKE			TL 0050		
	C SLOPE AND ZONE ARE CALCULATED AND RETURNED			TL 0060		
10	C S AND P MAKE UP THE TABLE			TL 0070		
	C N IS THE NUMBER OF VALUES IN THE TABLE			TL 0080		
	DO 1 I=1,N			TL 0090		
	IF (X.GE.S(I)).AND.(X.LT.S((I+1))) GO TO 2			TL 0100		
	CONTINUE			TL 0120		
15	1 SLOPE=(P(I+1)-P(I))/(S(I+1)-S(I))+.011			TL 0130		
	ZONE=P(I+1)-S(I)*S(I)			TL 0140		
	RETURN			TL 0150		
	F40			TL 0170		

APPENDIX C  
LISTING OF AIRPLANE DATA

- Boeing 727-100
- McDonnell Douglas C-9A
- AMST

AFFDL-TR-77-37

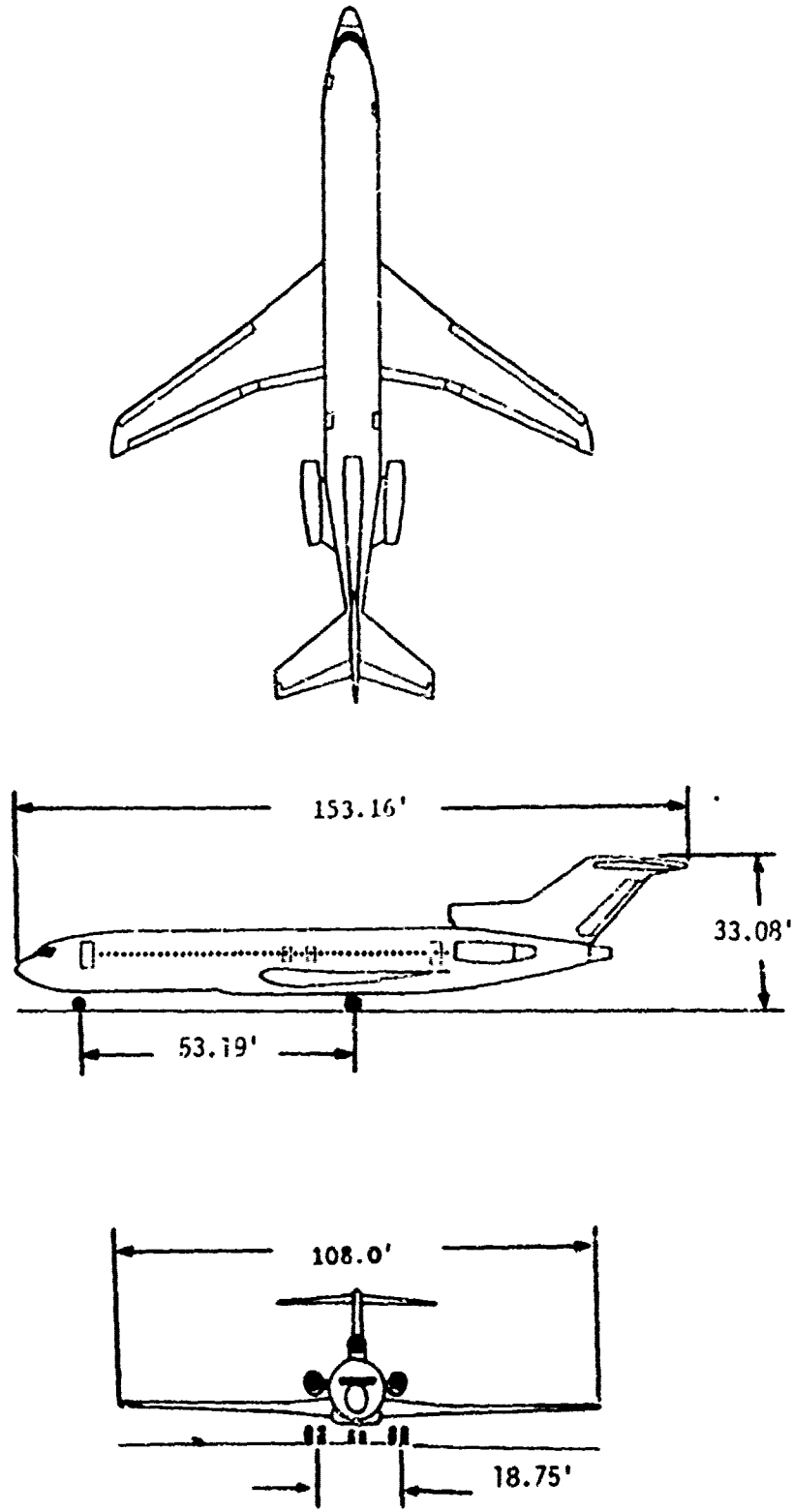


Figure C-1. Three View of Boeing 727-100

BEST AVAILABLE COPY

\*\*\*\*\* FOR F DATA \*\*\*\*\*

\*\*\*\*\* GENERAL AVAILABILITY DATA \*\*\*\*\*

301 FNG 727-130 16A-37 000005

W	106.000	1000	1313.77	0000	405.0.	A	70.673	0	465.703	W	32451706.
Sens	2.0	5.000	1.7	SLM	112.0	SLM	120.0	SLM	605.0	TALEMA	211.1
Actns	53.26	40.40	03.03	PAQH	205.03	VNOH	722.90	OANH	1.77	TSN	227.0.3L
Alt.	19.0	20.00	20.01	ABDHA	251.00	VCHH	223.90	OAH	.95	TSN	659.0.30
Cls.	312	500	.16	AFAT 194C.05	SP11H	50.0	THEUSI	19230.	TACOFF	252.30	
STANDBY MODE											
	2.725	4.315									
	2.465	4.315									
	3.097	3.403									
	11.920	1.303									
	15.423	1.303									
	12.027	1.303									
STANDBY MODE											
	7.325	1.655									
	10.022	1.655									
	12.721	1.655									
	16.300	1.655									

AFFDL-TR-77-37

BEST AVAILABLE COPY

hour	temp	sim05fr	sim05	sim04	sim03	sim02	sim01	checa	gen. mass
1	-0.3	-0.3	-0.27	-0.33	-0.36	-0.03	-0.03	6.6	
2	-0.29	-0.25	-0.24	-0.29	-0.06	-0.97	-0.97	7.6	
3	-0.17	-0.14	-0.22	-0.16	-0.26	-0.35	-0.35	2.7	
4	-0.27	-0.15	-0.12	-0.14	-0.12	-0.02	-0.02	1.1	
5	-0.12	-0.11	-0.11	-0.11	-0.12	-0.12	-0.12	1.9	
6	-0.21	-0.16	-0.13	-0.13	-0.14	-0.04	-0.04	5.0	
7	-0.15	-0.09	-0.08	-0.08	-0.09	-0.09	-0.09	3.6	
8	-0.03	-0.11	-0.12	-0.10	-0.06	-0.03	-0.03	17.6	
9	-0.09	-0.07	-0.07	-0.15	-0.13	-0.25	-0.25	25.1	
10	-0.05	-0.03	-0.04	-0.07	-0.16	-0.26	-0.26	11.5	

\*\*\*\*\* INITIAL CONDITIONS \*\*\*\*\*

Temp = -0.11; Pres = -0.473; Therate = -0.05742; Zeta = -13.573  
RH = 0.80; RH0 = -0.423; DuctTemp = -0.0163; DuctRate = -0.00051.

AFFDL-TR-77-37

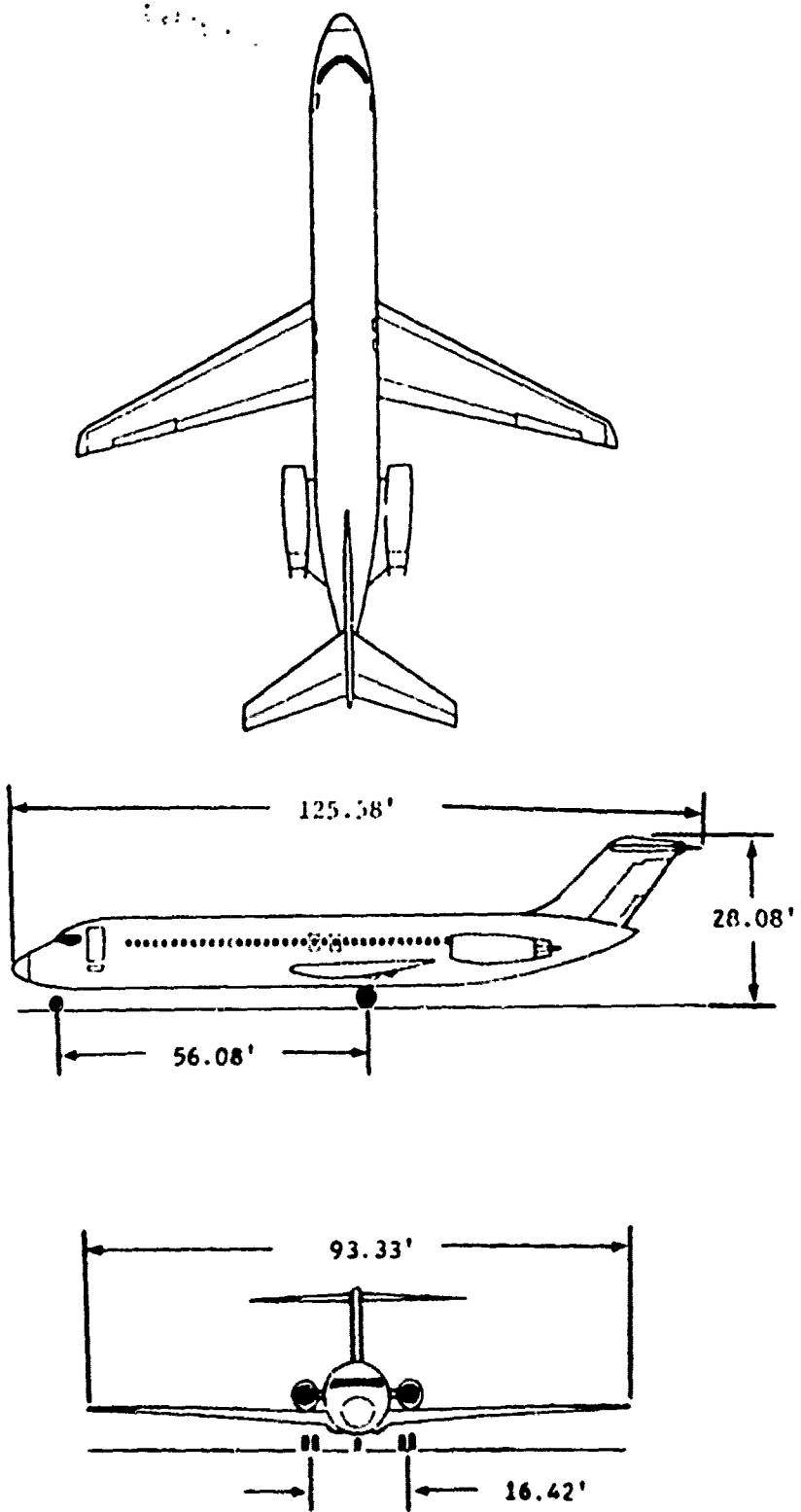


Figure C-2. Three View of McDonnell-Douglas C-9A

BEST AVAILABLE COPY

..... INPUT DATA .....

\*\*\*\*\* Original Aircraft DATA \*\*\*\*\*

C-130 148-114-00.

AC	Locality	Alt	Lat	Long	Altitude	Altitude	Altitude	Altitude	Altitude
3500	Do.	5200	100	0000	11000	40	11000	11000	11000
4410	East	4800	1600	4000	22000	0000	16000	16000	16000
7140	East	4800	0000	0000	12000	0000	12000	12000	12000
C-130	East	4800	0000	0000	12000	0000	12000	12000	12000
35000	West	0000	0000	0000	24000	0000	24000	24000	24000

STRUCTURE Wt's. P/M L/G/H/T.

10000	1000
4000	1000
7000	1000
12000	1000
12000	1000

STRUCTURE P/M L/G/H/T.

1000	1000
0000	1000
0000	1000
10000	1000
10000	1000

**BEST AVAILABLE COPY**

Model	Series	Sigma <sub>1</sub>	Sigma <sub>2</sub>	Sigma <sub>3</sub>	Sigma <sub>4</sub>	Sigma <sub>5</sub>	Sigma <sub>6</sub>	Center	Units, Mass
1	-0.15	-0.15	-0.17	-0.17	-0.17	-0.17	-0.17	13.51	0.2
2	-0.16	-0.17	-0.18	-0.18	-0.18	-0.18	-0.18	26.16	1.3
3	-0.09	-0.09	-0.10	-0.10	-0.10	-0.10	-0.10	55.75	21.2
4	-0.13	-0.12	-0.14	-0.14	-0.14	-0.14	-0.14	20.34	0.1
5	-0.08	-0.08	-0.09	-0.09	-0.09	-0.09	-0.09	33.96	2.0
6	-0.09	-0.09	-0.09	-0.09	-0.09	-0.09	-0.09	37.36	23.1
7	-0.09	-0.09	-0.09	-0.09	-0.09	-0.09	-0.09	37.36	23.1

Model	Series	Sigma <sub>1</sub>	Sigma <sub>2</sub>	Sigma <sub>3</sub>	Sigma <sub>4</sub>	Sigma <sub>5</sub>	Sigma <sub>6</sub>
1	-0.17	-0.17	-0.17	-0.17	-0.17	-0.17	-0.17
2	-0.17	-0.17	-0.17	-0.17	-0.17	-0.17	-0.17
3	-0.17	-0.17	-0.17	-0.17	-0.17	-0.17	-0.17
4	-0.17	-0.17	-0.17	-0.17	-0.17	-0.17	-0.17
5	-0.17	-0.17	-0.17	-0.17	-0.17	-0.17	-0.17
6	-0.17	-0.17	-0.17	-0.17	-0.17	-0.17	-0.17
7	-0.17	-0.17	-0.17	-0.17	-0.17	-0.17	-0.17

\*\*\*\*\* Initial Conditions \*\*\*\*\*

Temp = -21.113      Pres = -1.037      Inclination = 70.994      ZGel = -17.21-31.146.  
 Affine = -0.017      Ecc = -0.005      Reaction = 0.000      d.Gel = -99.96.

AFFDL-TR-77-37

BEST AVAILABLE COPY

\*\*\*\*\* INPUT DATA \*\*\*\*\*

\*\*\*\*\* GENERAL AERODYNAMIC DATA \*\*\*\*\*

AET 150922Z 01:

Alt	193000.0	400	1172.0	0.0	435.0	4.0	0.3550	7.0	627.50	4.0	113.22	0.0	2516320.0
SFCM	2.0	5.0	1.0	0.0	0.0	0.0	0.0	0.0	0.0	0.0	0.0	0.0	0.0
4000	70.0	4.0	5.0	0.0	0.0	0.0	0.0	0.0	0.0	0.0	0.0	0.0	0.0
8000	23.75	3.0	4.0	1.0	0.0	0.0	0.0	0.0	0.0	0.0	0.0	0.0	0.0
Cls	2.050	0.7	0.651	0.0	0.0	0.0	0.0	0.0	0.0	0.0	0.0	0.0	0.0
Stress Mod	0.000	0.000	0.000	0.000	0.000	0.000	0.000	0.000	0.000	0.000	0.000	0.000	0.000
5.000	0.075	0.075	0.075	0.075	0.075	0.075	0.075	0.075	0.075	0.075	0.075	0.075	0.075
6.000	0.100	0.100	0.100	0.100	0.100	0.100	0.100	0.100	0.100	0.100	0.100	0.100	0.100
11.200	0.032	0.032	0.032	0.032	0.032	0.032	0.032	0.032	0.032	0.032	0.032	0.032	0.032
16.000	0.022	0.022	0.022	0.022	0.022	0.022	0.022	0.022	0.022	0.022	0.022	0.022	0.022
18.000	0.015	0.015	0.015	0.015	0.015	0.015	0.015	0.015	0.015	0.015	0.015	0.015	0.015
22.000	0.010	0.010	0.010	0.010	0.010	0.010	0.010	0.010	0.010	0.010	0.010	0.010	0.010
25.000	0.008	0.008	0.008	0.008	0.008	0.008	0.008	0.008	0.008	0.008	0.008	0.008	0.008
28.000	0.006	0.006	0.006	0.006	0.006	0.006	0.006	0.006	0.006	0.006	0.006	0.006	0.006
30.000	0.004	0.004	0.004	0.004	0.004	0.004	0.004	0.004	0.004	0.004	0.004	0.004	0.004

BEST AVAILABLE COPY

the first time in the history of the country.

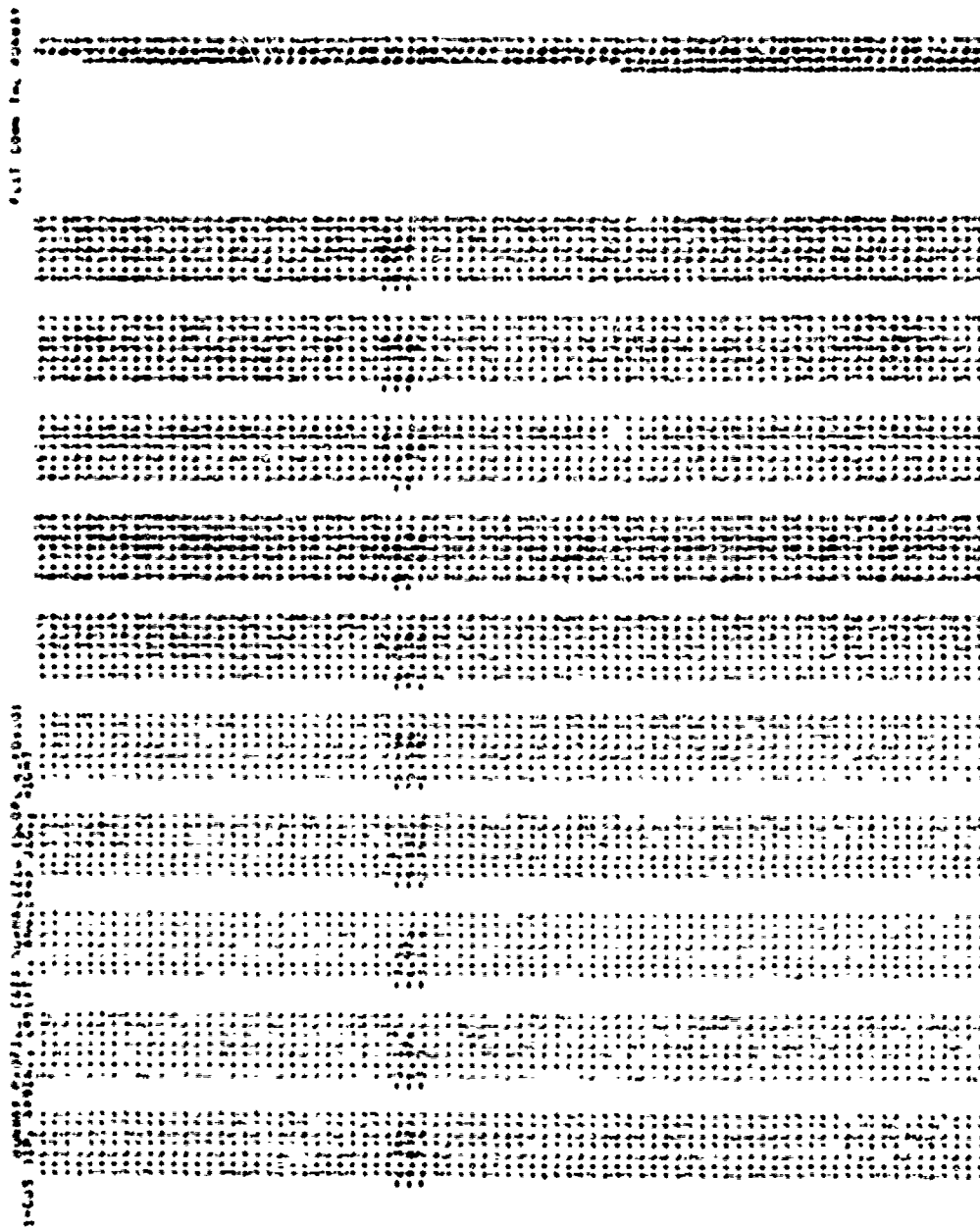
APPENDIX D  
LISTING OF RUNWAY PROFILES

1. Figure D-1 - Washington National Runway 36-Left, Center, and Right hand profiles:
2. Profile data listing of the 1-cos dip used in these simulations:  
All three lines of profile were identical except that they occur at different times corresponding to the gear locations.

AFFDL-TR-77-37

**Figure D-1. Washington National Runway 36 with Linear Trend Removed**

**BEST AVAILABLE COPY**



BIBLIOGRAPHY

Butterworth, C. K., and Boozer, D. E., Jr., C-141A Computer Code for Runway Roughness Studies, AFWL-TR-70-71, Air Force Weapons Laboratory, Kirtland AFB, New Mexico, August 1970.

Chance Vought Corporation, A Rational Method for Predicting Alighting Gear Dynamic Loads, ASD-TDR-62-555, Aeronautical Systems Division, Wright-Patterson AFB, Ohio, December 1963.

Cook, Robert F., Use of Discrete Runway Profile Elevation Data in Determining the Dynamic Response of Vehicles, TM-68-3-FDDS, Air Force Flight Dynamics Laboratory, Wright-Patterson AFB, Ohio, May 1968.

Crenshaw, B. M., and Butterworth, C. K., Lockheed Georgia Company, Aircraft Landing Gear Dynamic Loads from Operation on Clay and Sandy Soil, AFFDL-TR-69-51, Air Force Flight Dynamics Laboratory, Wright-Patterson AFB, Ohio, February 1971.

NACA TN 2477, Investigation of the Air-Compression Process During Drop Tests of an Oleo-Pneumatic Landing Gear, 1951.

Quade, Delmar A., The Boeing Company, Wichita Division, Location of Rough Areas of Runways for B-52 Aircraft, AFFDL-TR-67-175, Air Force Flight Dynamics Laboratory, Wright-Patterson AFB, Ohio, March 1968.

REFERENCES

1. Goldman, D. E., and von Gierke, H. E., 'Effects of Shock and Vibration on ...', Volume III, Chap. 44, Shock and Vibration Handbook (C. M. Harris and C. E. Crede, editors) McGraw Hill Book Co., New York, 1961.
2. Gerardi, A. G., Lohwasser, A. K., Computer Program for the Prediction of Aircraft Response to Runway Roughness, AFWL-TR-73-109, Volume I and II, Air Force Weapons Laboratory, Kirtland AFB, New Mexico, September 1973.